CEMRACS 2016: PAMiFLU

Parallel adaptive multiresolution methods for fluid and plasma flows

- What do we do?
  - Wavelet based regularization of incompressible 3d Euler equations
  - Immersed boundary methods for inhom. Neumann bc
  - Higher order local time stepping for adaptive MR methods
- Who are we?
  - Margarete Domingues, Odim Mendes, INPE, Brazil
  - Marie Farge, ENS Paris, France
  - Naoya Okamoto, Nagoya University, Japan
  - Kai Schneider, I2M, Aix-Marseille University, France
- Un grand merci to the organizers of CEMRACS 2016
- *PhD opening, ANR-DFG project AIFIT*

INSTITUT DE MATHÉMATIQUES de MARSEILLE

Faculté des Sciences Aix-Marseille Université

Aix-Marseille université

cnrs

Bumblebees in Turbulence:

massively parallel numerical simulations

Kai Schneider

I2M, Aix-Marseille Université, France

CEMRACS 2016

Numerical challenges in parallel scientific computing

CIRM, Luminy

August 18th, 2016, Marseille, France

Aix*Marseille université

熊蜂

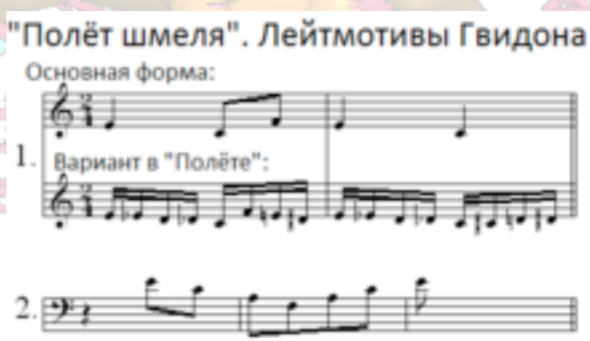

N. Rimski Korsakow. 1899

Acknowledgements

- **Thomas Engels** (Berlin/Marseille, Germany/France)
- Marie Farge (Paris, France)
- Dmitry Kolomenskiy (Chiba, Japan)
- Fritz-Olaf Lehmann (Rostock, Germany)
- Romain Nguyen van yen (Toulouse, France)
- Joern Sesterhenn (Berlin, Germany)

Thomas Engels

Dmitry Kolomenskiy

Motivation


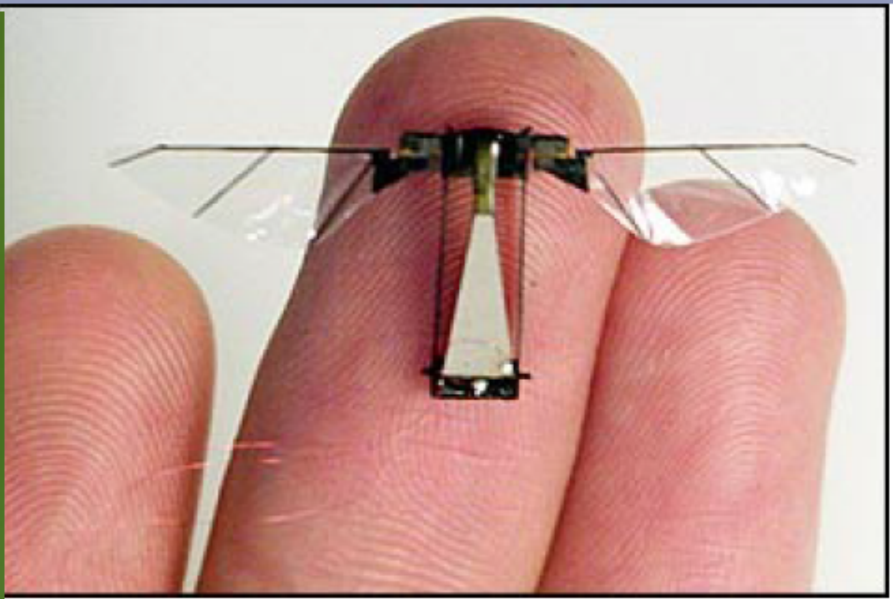


Outline

- Motivation
- The volume penalization method: a simple 1d example
- Part I: Numerical method
  - Navier-Stokes meets penalization
- Part II: Application to insect flight
  - Bumblebee flight in turbulence
- Part III: Application to swimming
  - Chordwise flexible pitching foils
- Conclusions

Motivation

- Solving PDEs (Navier-Stokes, Maxwell eq., heat eq., convection-diffusions, Poisson eq., Laplace eq.) in complex geometries using numerical methods.
- Different solutions available:
  - Body fitted grids.
  - Mapping techniques.
  - Immersed boundary methods/ fictitious domain methods (direct forcing, Lagrangian multipliers, penalty techniques, …)
- Here volume penalization technique.
- A review paper: K. Schneider. Immersed boundary methods for numerical simulation of confined fluid and plasma turbulence in complex geometries: a review. *J. Plasma Phys.*, 81(6), 435810601, 2015. arXiv:1508.04593

Initial Boundary Value Problem in complex geometry

$$Lu = f \quad \text{for} \quad x \in \Omega_f$$

with $bu = g$ at $\partial\Omega_f$ (Plus initial conditions)

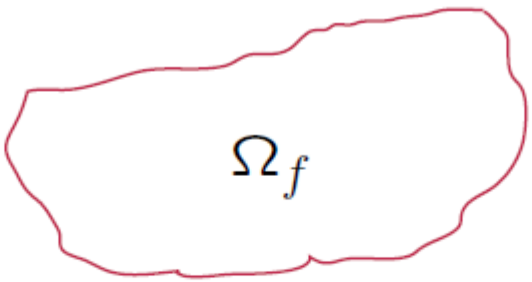

with *L* being, e.g. the Laplace operator, or Navier-Stokes or Maxwell operator

Penalized problem in simple geometry

$$Lu_\eta = f - \frac{1}{\eta}\chi(bu - g) \quad \text{for} \quad \boldsymbol{x} \in \Omega = \Omega_f \cup \Omega_s$$

Penalization (modeling) error: $\| u - u_\eta \| \propto \eta^\alpha$

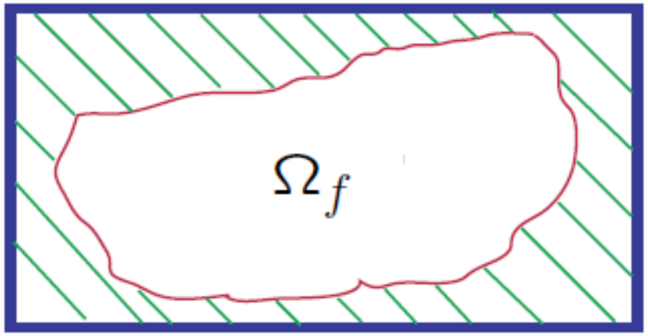

Discretized penalized problem

$$L^N u_\eta^N = f^N - \frac{1}{\eta}\chi^N(bu - g) \quad \text{for} \quad \boldsymbol{x} \in \Omega$$

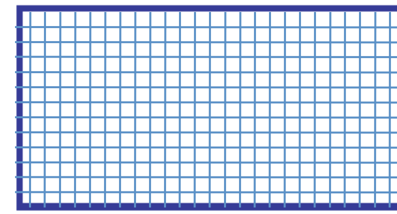

with $\triangle x \propto 1/N$

Discretization error: $\| u_\eta - u_\eta^N \| \propto \left(\frac{1}{N}\right)^\beta$

Total error = modeling error + discretization error

$$\| u - u_\eta^N \| \leq \| u - u_\eta \| + \| u_\eta - u_\eta^N \|$$

Some analysis: a simple example

Let us consider the one-dimensional Poisson equation

$$-\frac{\mathrm{d}^2 w(x)}{\mathrm{d}x^2} = f(x)$$

with $x \in \Omega =]0, \pi[$, homogeneous Dirichlet boundary conditions

$$w(0) = 0, \quad w(\pi) = 0$$

and the right-hand side given by a sinusoidal function

$$f(x) = m^2 \sin mx.$$

The exact solution to this problem is

$$w(x) = \sin mx.$$

Exact solution of the penalized 1d Poisson equation

Let us now solve this problem approximately using the volume penalization method. The domain is extended to $\mathbb{T} = \mathbb{R}/2\pi\mathbb{Z}$. The Poisson equation is modified by adding the penalization term,

Penalization term

$$-v'' + \frac{1}{\eta}\chi v = f, \tag{5}$$

where $''$ denotes the second derivative with respect to x, f is extended naturally through $\mathbb{T}$ using the original formula (3) and the mask function is

$$\chi = \begin{cases} 0, & x \in]0,\pi[\\ 1/2, & x = 0,\ x = \pi \\ 1, & x \in]\pi, 2\pi[\end{cases} \tag{6}$$

Periodic boundary conditions are imposed at $x = 0$ and $x = 2\pi$. The exact solution to the penalized problem is

$$v(x) = \begin{cases} \sin mx + A_1 x + A_2, & x \in [0,\pi[\\ \frac{m^2\eta}{1+\eta m^2} \sin mx + B_1 e^{-x/\sqrt{\eta}} + B_2 e^{x/\sqrt{\eta}}, & x \in [\pi, 2\pi[\end{cases} \tag{7}$$

Exact solution of the penalized 1d Poisson equation

v(x) *v'(x)* *v''(x)*

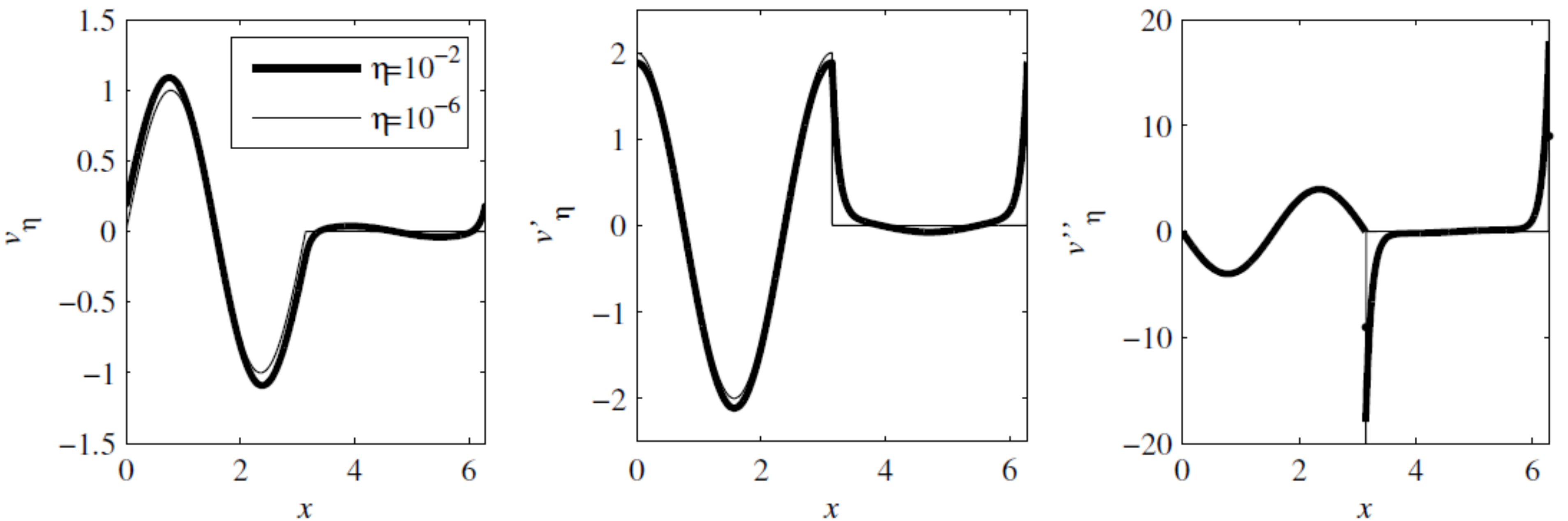

Exact penalized solution (left) for *m*=2 and its first (center) and second (right) derivatives.

Penalization error of the Dirichlet problem

Using the exact solution of the penalized problem the leading order L^2 error with respect to the Dirichlet problem is given by

$$\varepsilon_1 \sim \frac{m\sqrt{2-(-1)^m}}{\sqrt{6}}\sqrt{\eta} \quad \text{as} \quad \eta \to 0$$

where the $\sqrt{\eta}$ behavior is consistent with previous studies by Angot et al., 1999 and Carbou and Fabrie, 2003.

Aix*Marseille université

Discretization error of the penalized equation

The penalized problem is discretized with a pseudospectral Fourier method using N grid points. For the L^2 error between the discrete solution and the exact solution of the penalized problem we get,

$$\varepsilon_2 \sim K \frac{m\pi^{3/2}}{3\sqrt{2}} \frac{1}{\sqrt{\eta}N^2} \quad \text{as} \quad \eta \to 0, \quad \sqrt{\eta}N^2 \to \infty,$$

where K=2 for m even and $K \approx 3.84$ for m odd.
The N^{-2} behavior is related to the regularity the exact penalized solution as observed by Min & Gottlieb 2003 for elliptic equations with discontinuous coefficients.

How to choose η?

Combining the two estimates we get a bound for the total error ε between the discrete-penalized solution and the exact solution of the Dirichlet problem:

$$\varepsilon \leq \varepsilon_1 + \varepsilon_2 \sim \frac{m\sqrt{2-(-1)^m}}{\sqrt{6}}\sqrt{\eta} + K\frac{m\pi^{3/2}}{3\sqrt{2}}\frac{1}{\sqrt{\eta}N^2} \quad \text{as} \quad \eta \to 0, \quad \sqrt{\eta}N^2 \to \infty$$

When η is chosen with the right order of magnitude, i.e. $\eta \propto 1/N$, in order to optimize the preceding estimate, then the resulting error is

$$\varepsilon \propto \frac{1}{N}$$

which suggests that the penalization method with Fourier discretization is a first order method.

Aix*Marseille université

Convergence of the Fourier collocation method

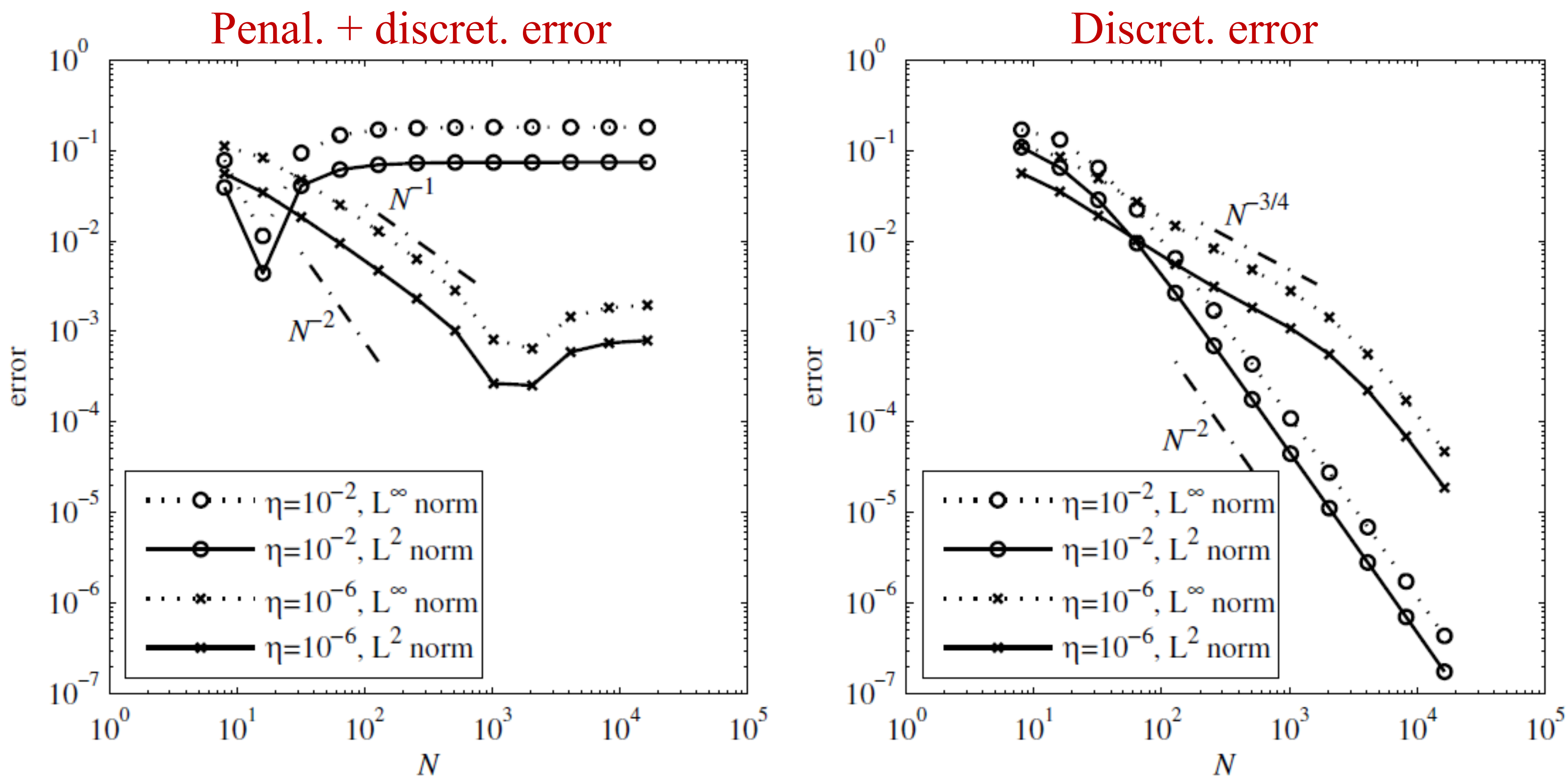

Error with respect to the exact Dirichlet solution in the interior of the fluid domain (left) and with respect to the penalized solution in the whole domain (right).

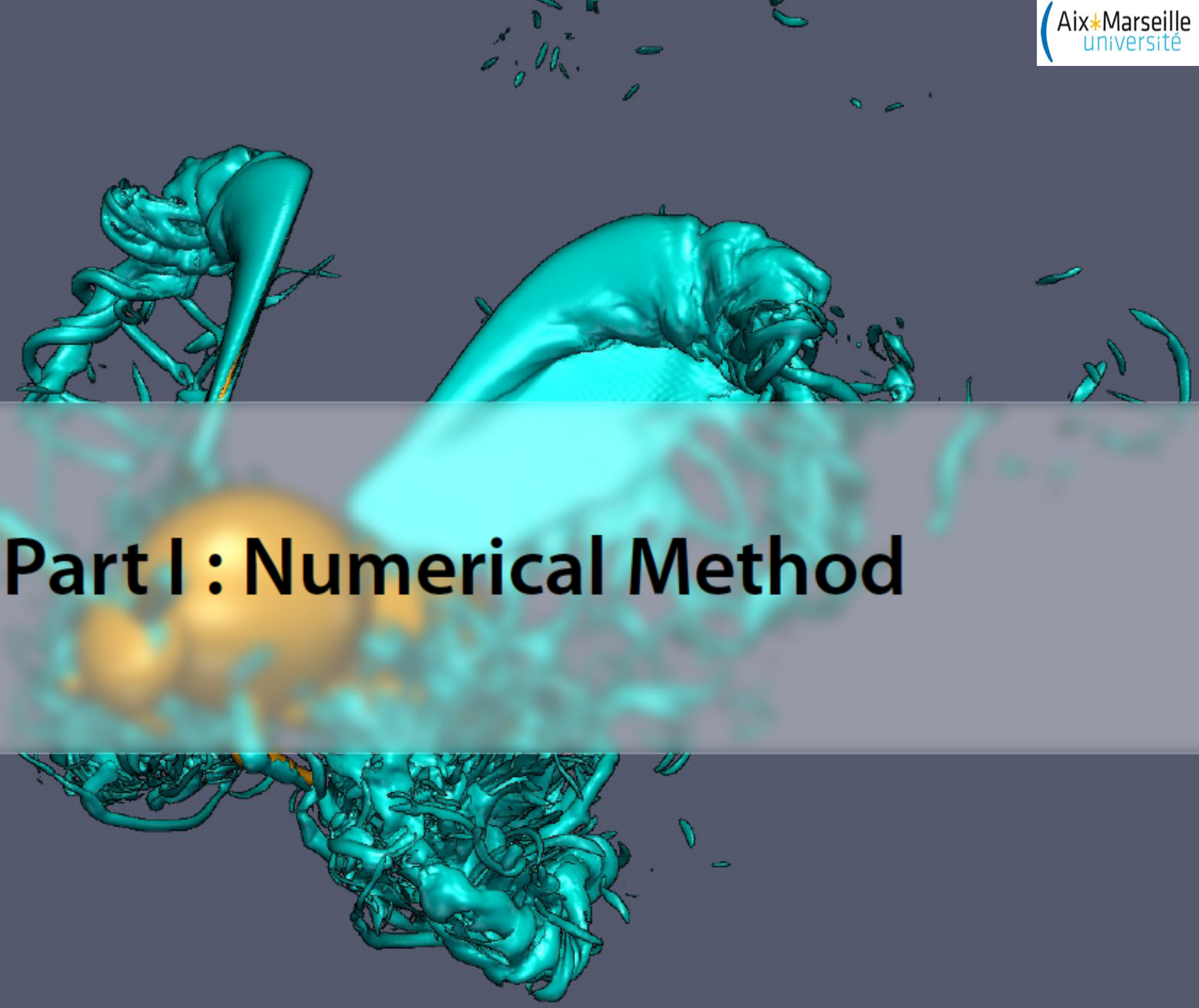

Part I : Numerical Method

Volume penalization method

Penalized incompressible Navier-Stokes eqn.:

$$\begin{aligned} \partial_t \underline{u} + \underline{\omega} \times \underline{u} &= -\nabla \Pi + \nu \nabla^2 \underline{u} + \underline{F}_p - \frac{\chi}{C_\eta} \left(\underline{u} - \underline{u}_s \right) \\ \nabla \cdot \underline{u} &= 0 \\ \underline{u} \left(\underline{x}, t = 0 \right) &= \underline{u}_0 \left(\underline{x} \right) \end{aligned}$$

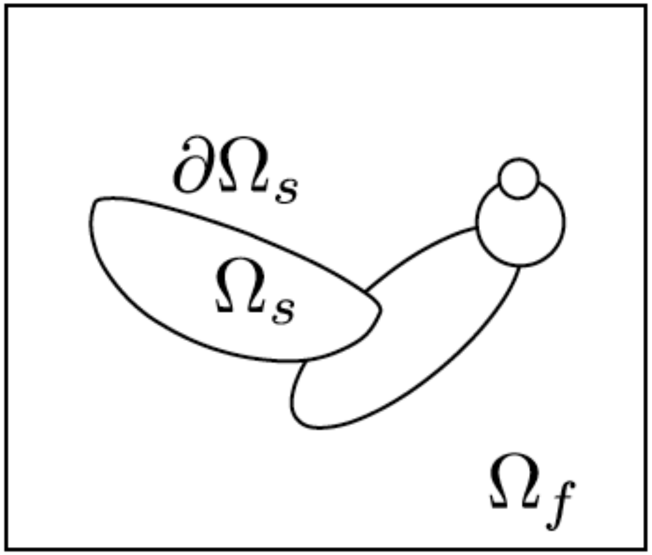

No-slip BC through penalization

$$\chi \left(\underline{x}, t \right) = \begin{cases} 0 & \text{if } \underline{x} \in \Omega_f \\ 1 & \text{if } \underline{x} \in \Omega_s \end{cases}$$

P. Angot and C. Bruneau and P. Fabrie, "A penalization method to take into account obstacles in incompressible viscous flows", Numer. Math. 81 (1999)

Mask Function

- If the obstacle moves or deforms, a smoothed mask function is used
- Use signed distance function $\delta(\underline{x})$
- Then the mask function is:

$$\chi(\delta) = \begin{cases} 1 & \delta \leq -h \\ \frac{1}{2}\left(1 + \cos\left(\pi \frac{\delta + h}{2h}\right)\right) & -h < \delta < +h \\ 0 & \delta > +h \end{cases}$$

works also for flexible, moving obstacles

Engels, T.; Kolomenskiy, D.; Schneider, K. & Sesterhenn, J. Numerical Simulation of Fluid-Structure Interaction with the Volume Penalization Method J. Comput. Phys., 2015, 281, 96-115

Discretization

- Space: Fourier Pseudospectral
  - Easy & precise differentiation in Fourier space
  - Laplace operator diagonal: no linear system for Poisson eqn.
  - Suitable for large scale supercomputers
- Time: Adams-Bashforth with integrating factor
  - No restriction from viscosity
  - 2^{nd} order enough (small time steps anyways)

Vorticity Sponge

- Remove periodicity with vorticity sponge:

$$\partial_t \underline{u} + \underline{\omega} \times \underline{u} = -\nabla \Pi + \nu \nabla^2 \underline{u} - \frac{\chi}{C_\eta}\left(\underline{u} - \underline{u}_s\right) - \nabla \times \frac{\left(\frac{\chi_{sp}}{C_{sp}}\left(\underline{\omega} - \underline{\omega}_0\right)\right)}{\nabla^2}$$

- Is divergence-free and of zero mean flow

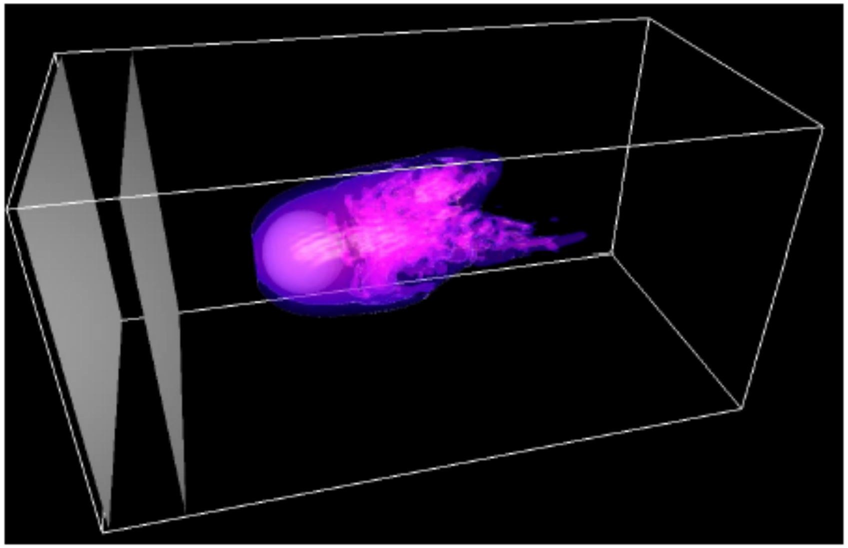

insect_rigid_turb.avi

Code Aspects: FluSI

- Open source:
  github.com/pseudospectators/FLUSI
- Modular structure
- Equidistant Cartesian grids
- MPI-Parallel
- Good scaling

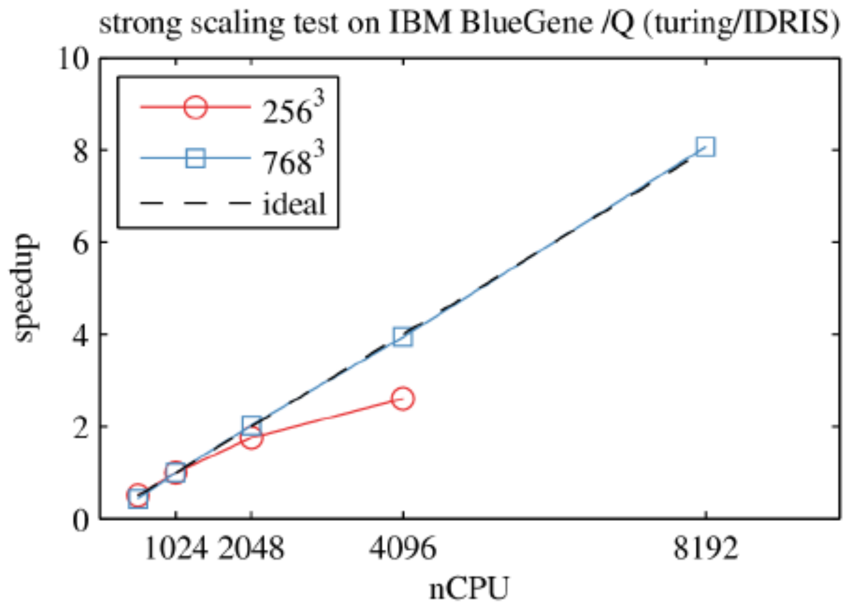

Engels, T.; Kolomenskiy, D.; Schneider, K. & Sesterhenn, J. FluSI: A novel parallel simulation tool for flapping insect flight using a Fourier method with volume penalization arXiv:1506.06513, 2015, ~~under consideration for~~ SIAM J. Sci. Comput. accepted

Application to

2d confined turbulence

2D decaying turbulence in a circular domain

Mask:

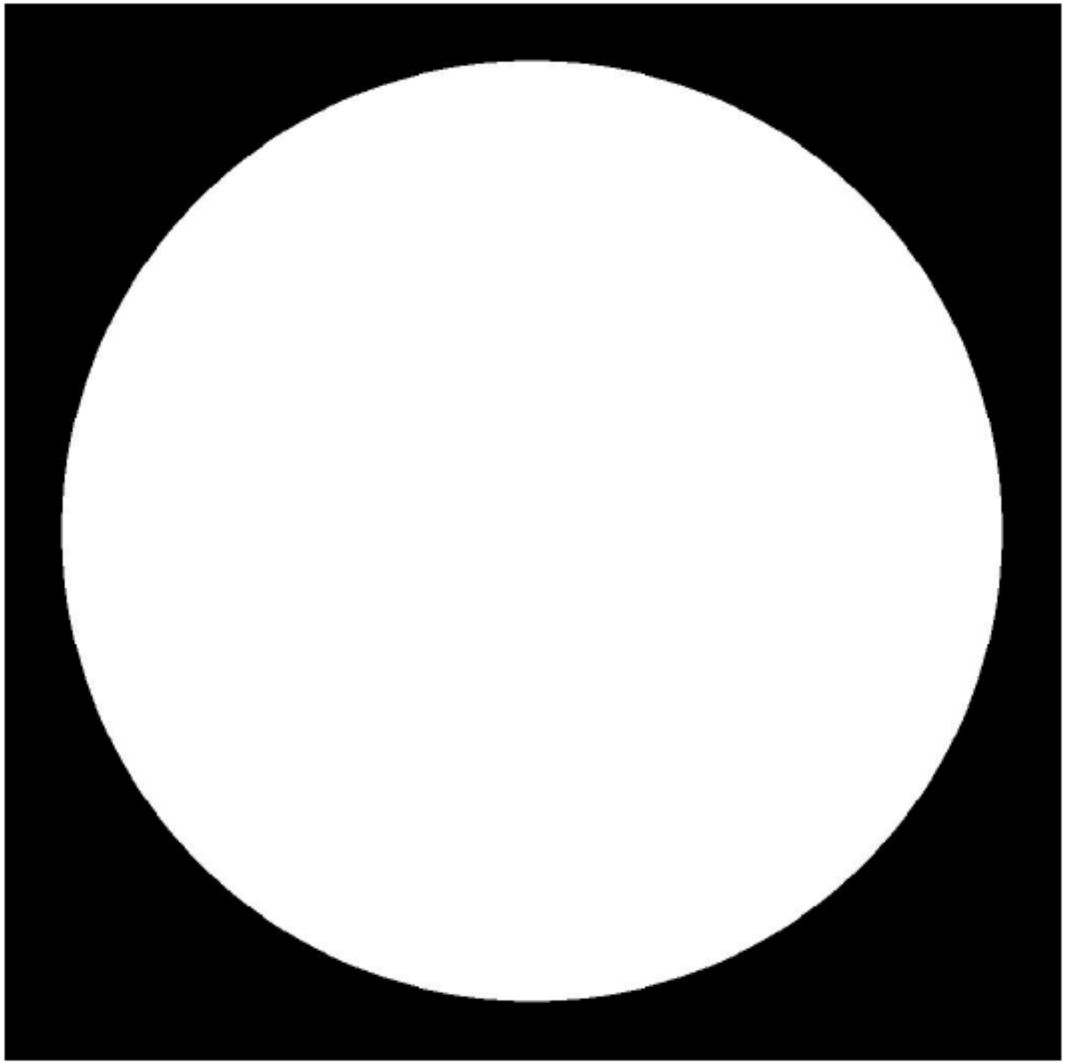

2d decaying turbulence in a circular domain

Vorticity,
N=1024^2

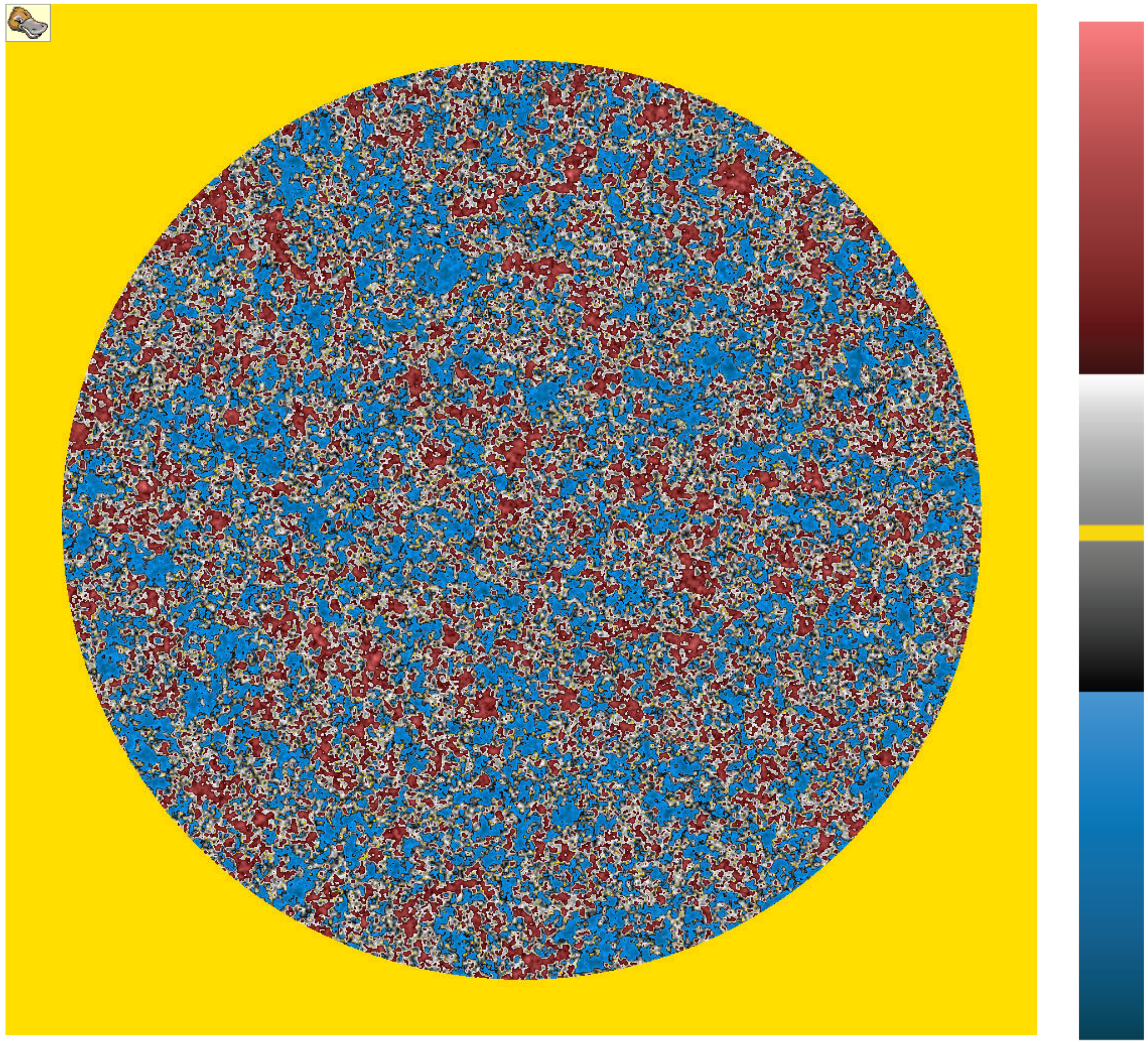

Ref.: K. Schneider and M. Farge, *Phys. Rev. Lett.*, 95(24), 2005

2D decaying turbulence in a circular domain

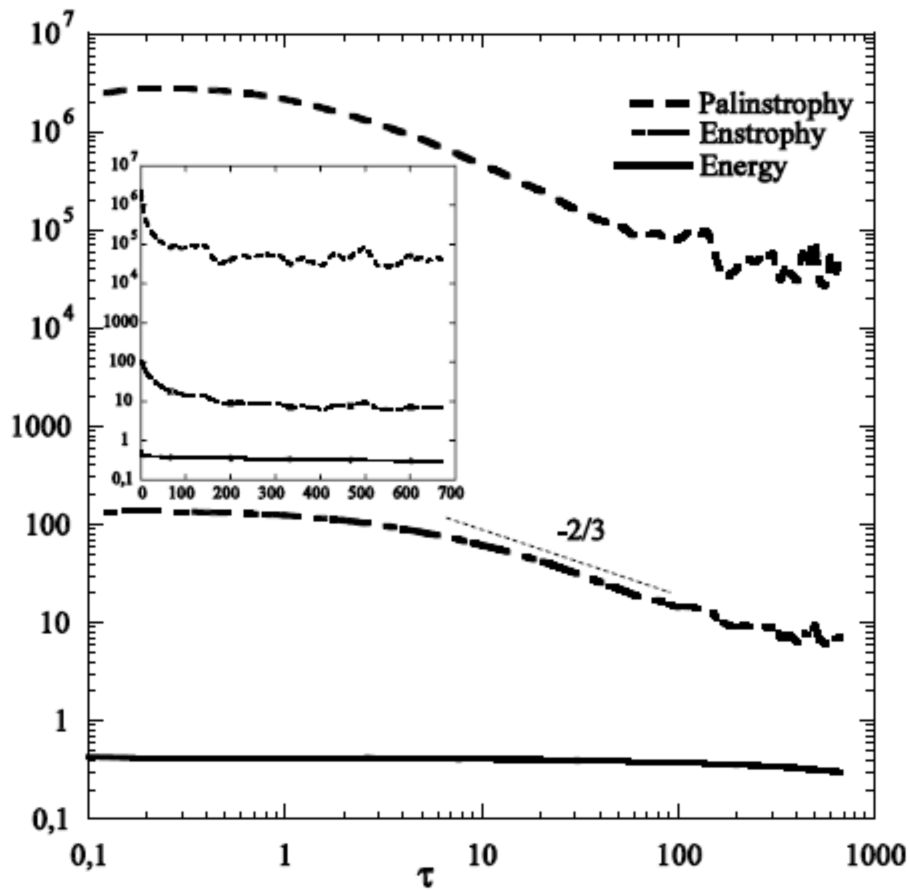

Time evolution of energy E, enstrophy Z and palinstrophy P.

Part II : FSI with rigid objects
Application to insect flight

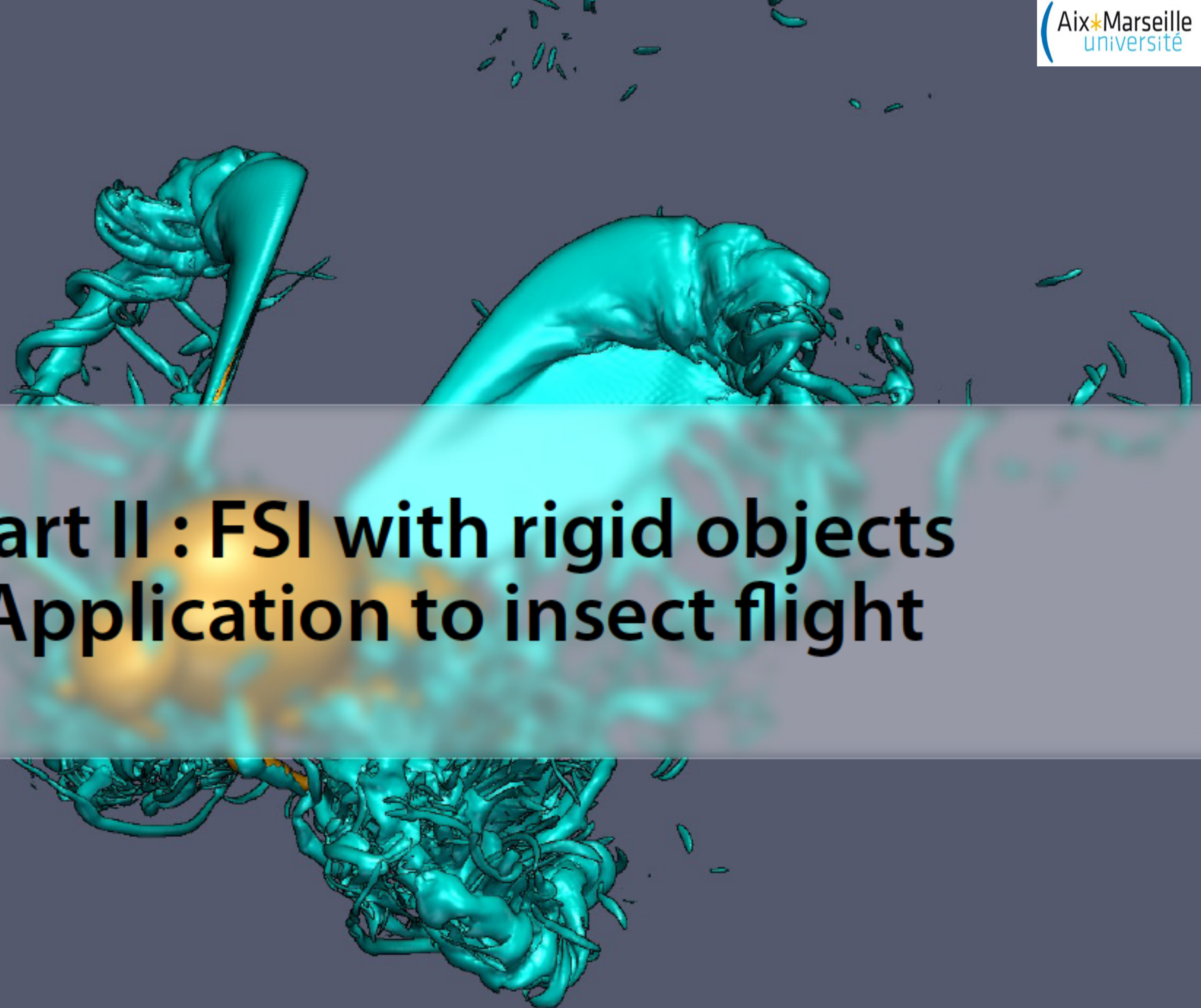

Aix*Marseille université

Model Assumptions

- Rigid wings → flexible in the future
- Include body, legs, antennae etc.
- Possibly free flight (1-6 DoF)
- tethered flight (0 DoF, fixed)

Insect Model: Kinematics

12 parameters (x, z, y, yaw, pitch, roll; feathering, positional, deviation)

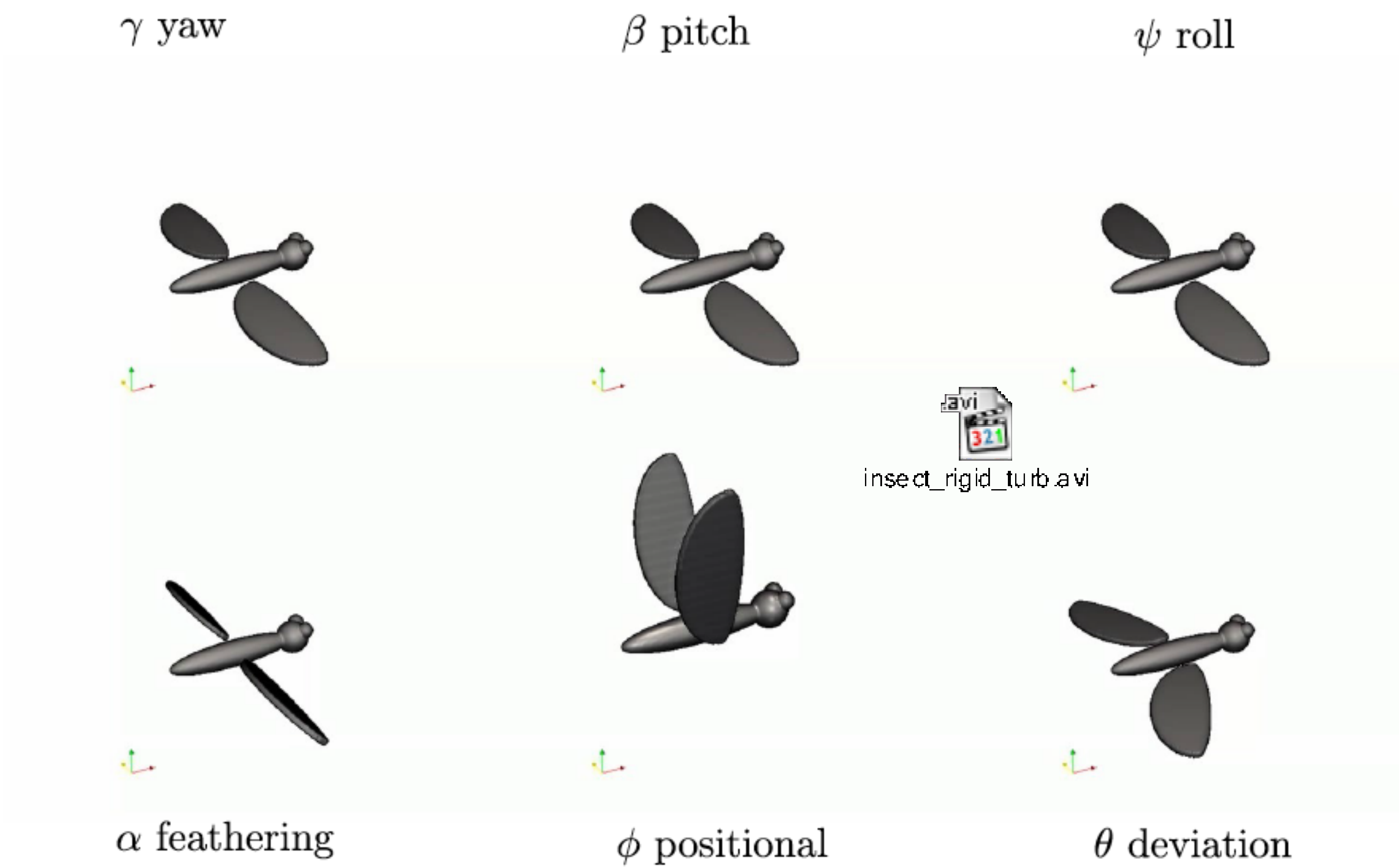

Kinematics of a fruitfly (hovering)

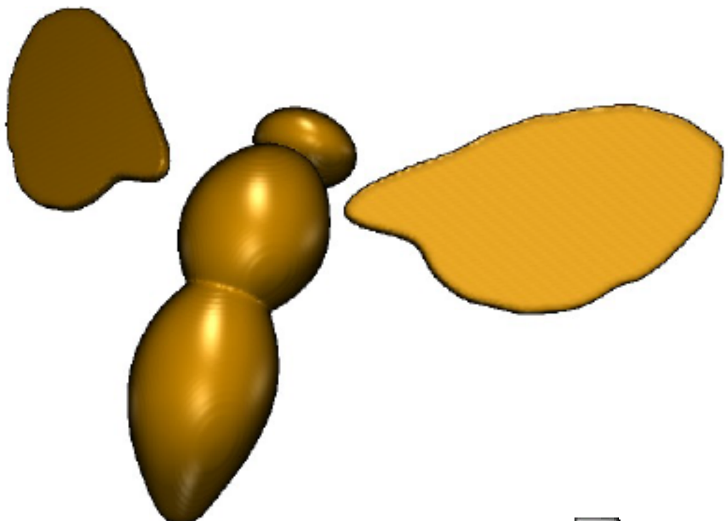

insect_rigid_turb.avi

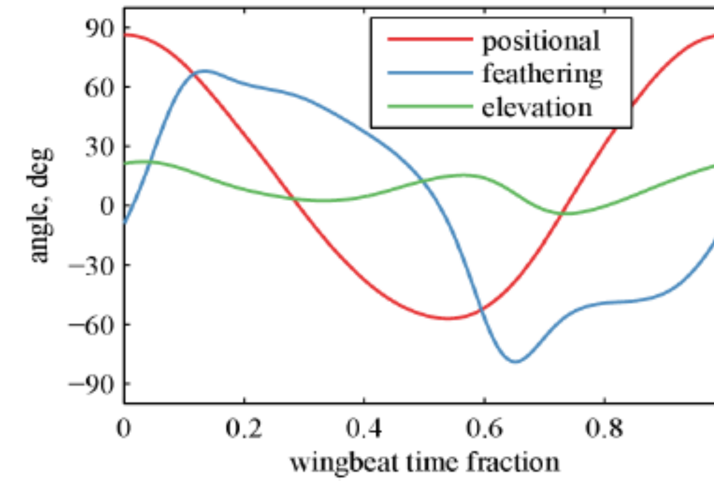

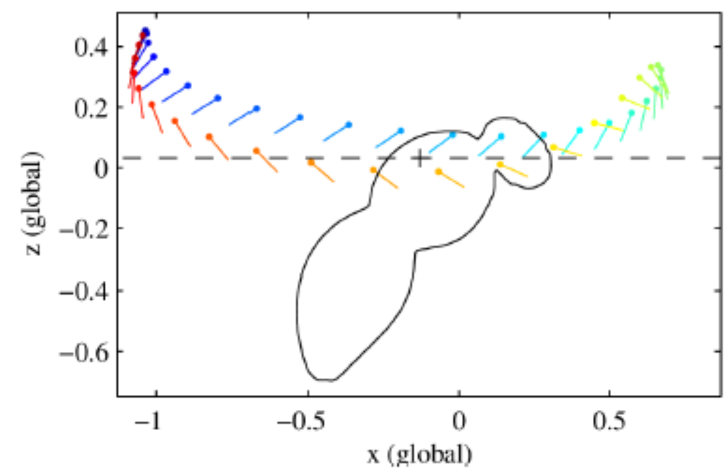

Validation: Comparison Maeda et al.

M. Maeda and H. Liu, "Ground effect in fruit fly hovering: A three-dimensional computational study.", J. Biomech. Sc. Engin. (2013)

Differences: 3.26% (lift) and 1.00% (power) during last stroke

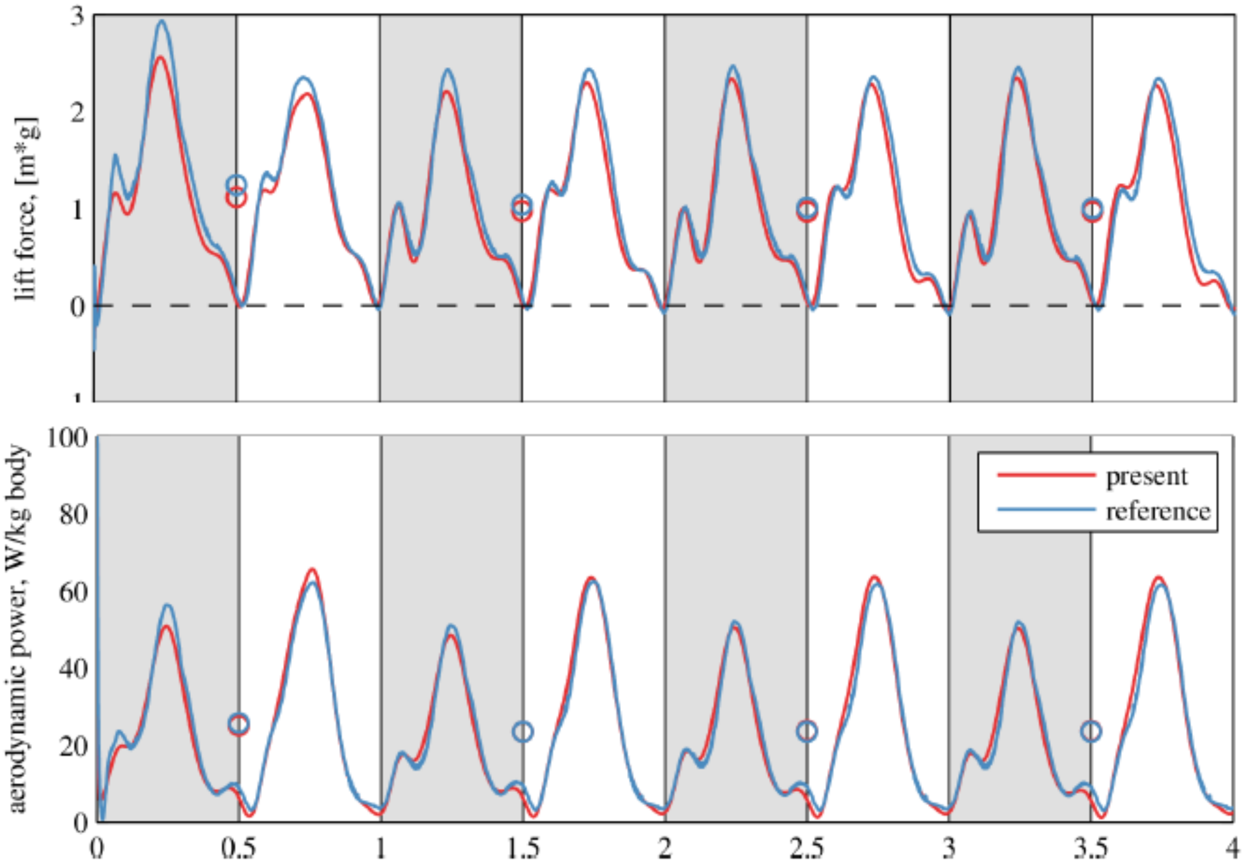

Bumblebee flight in turbulence

Bumblebee in turbulence

- Motivation: outdoors environment highly turbulent
- Until now almost all studies consider clean laminar inflow, all exceptions are experimental work

  S. A. Combes and R. Dudley, "Turbulence-driven instabilities limit insect flight performance", PNAS 106 (2009)

  S. Ravi and J.D. Crall and A. Fisher and S. A. Combes, "Rolling with the flow: bumblebees flying in unsteady wakes", J. Exp. Biol. 216 (2013)

  Hummingbirds: Ortega-Jimenez 2013, 2014 ; Ravi 2015

- No numerical work yet

  T. Engels and D. Kolomenskiy and K. Schneider and J. Sesterhenn and F.-O. Lehmann, "Bumblebee flight in heavy turbulence", Phys. Rev. Letters, 116, 028103, 2016.

- We first consider laminar inflow as reference

Bumblebee Model

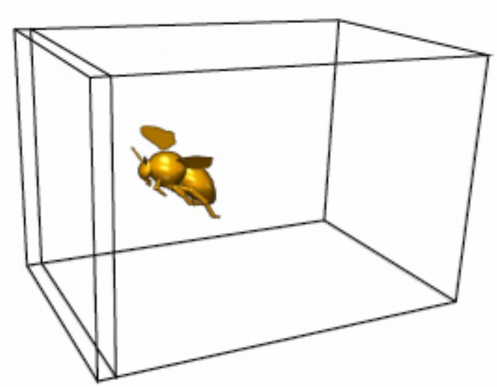

- Based on Dudley and Ellington 1990
- Consider forward flight at 2.5 m/s
- Wing length R = 13.2mm
- Frequency f = 152Hz
- Reynolds Re = $U_{tip}R/\nu$ = 2042 where $U_{tip} = 2\pi\Phi f c_m$
- Resolution 1152x768x768 (680M) on a domain of 6R x 4R x 4R, C_η=2.5e-4

Bumblebee Model: Geometry

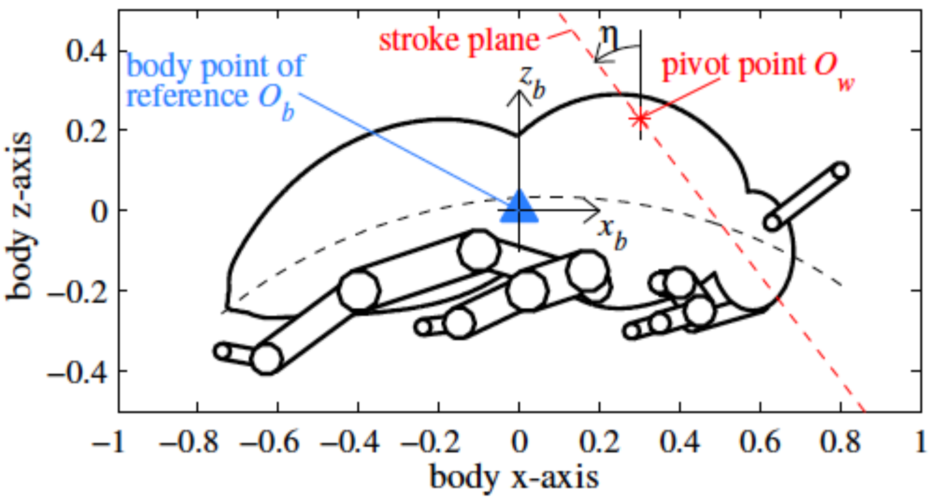

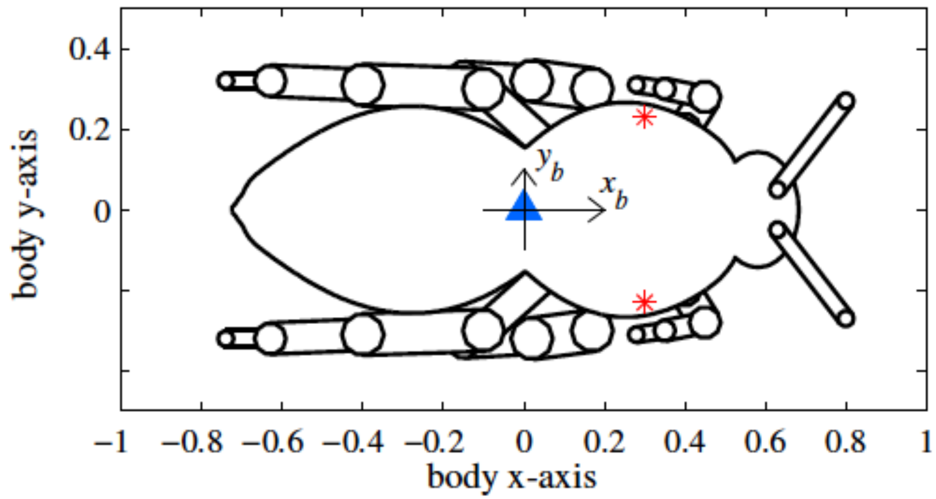

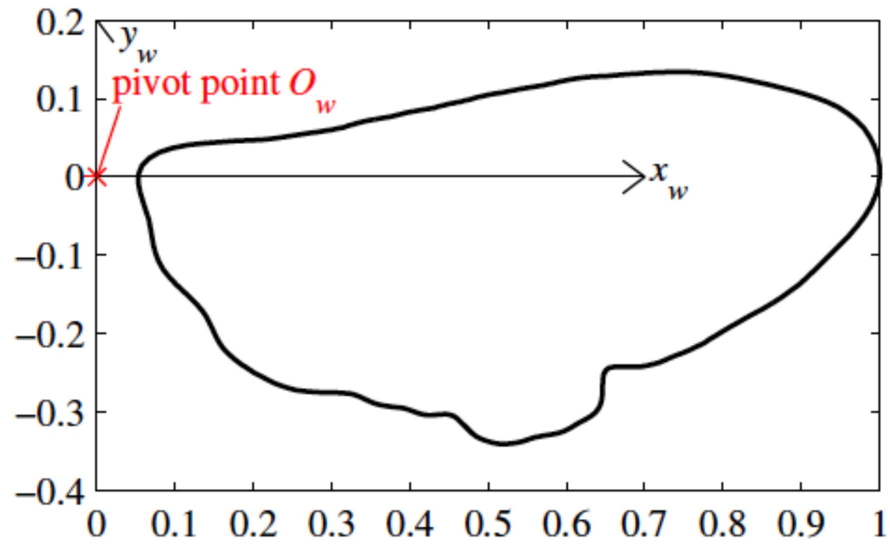

Bumblebee Model : Kinematics

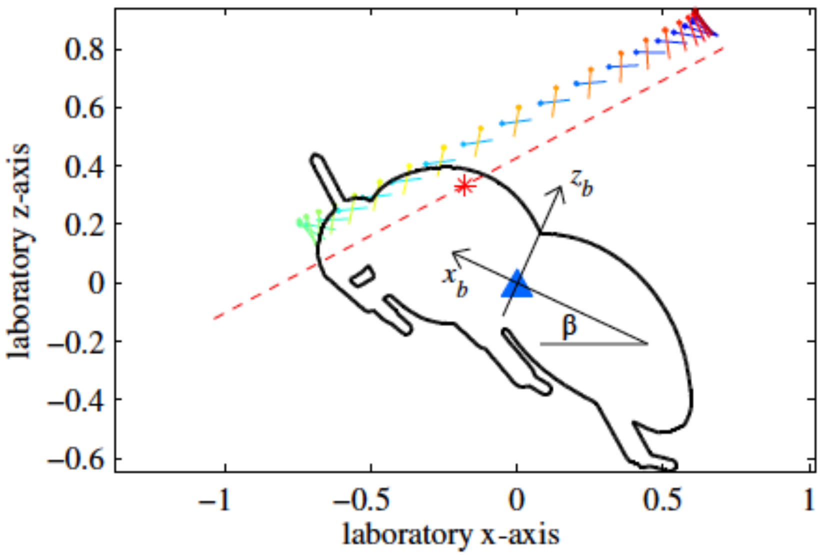

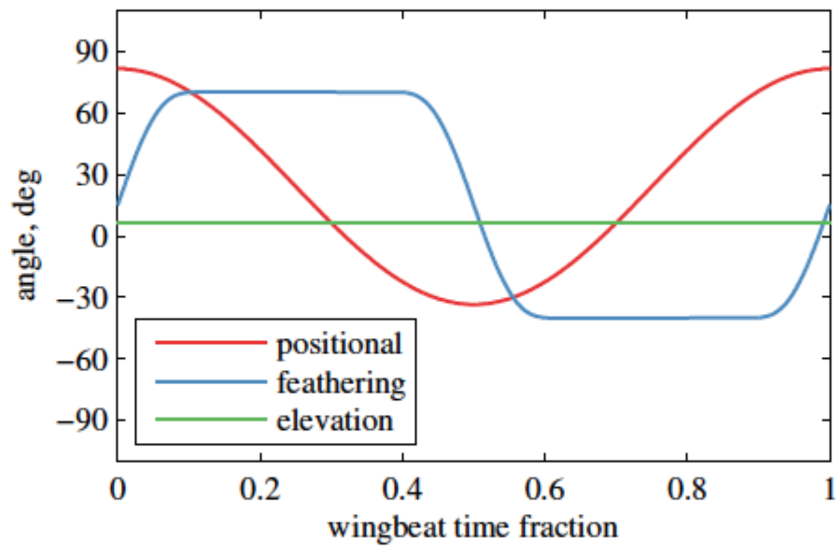

Kinematics are derived from [1] with simplifications introduced in [2], adopted to our model to obtain balanced flight

[1] Dudley, R. & Ellington, C. P. Mechanics of forward flight in bumblebees I. Kinematics and morphology J. Exp. Biol., 1990, 148, 19-52

[2] Xu, N. & Sun, M. Lateral dynamic flight stability of a model bumblebee in hovering and forward flight J. Theor. Biol., 2013, 319, 102-115

Laminar Inflow

Stroke averaged values for laminar inflow:

Forward force F_h	-0.08	[weight]
Vertical force F_v	1.02	[weight]
Aerodynamic power P_{aero}	84.05	[W/kg body]
Moment M_x (roll)	0.00	[weight $\cdot$ R]
Moment M_y (pitch)	0.01	[weight $\cdot$ R]
Moment M_z (yaw)	0.00	[weight $\cdot$ R]

Wake turbulence

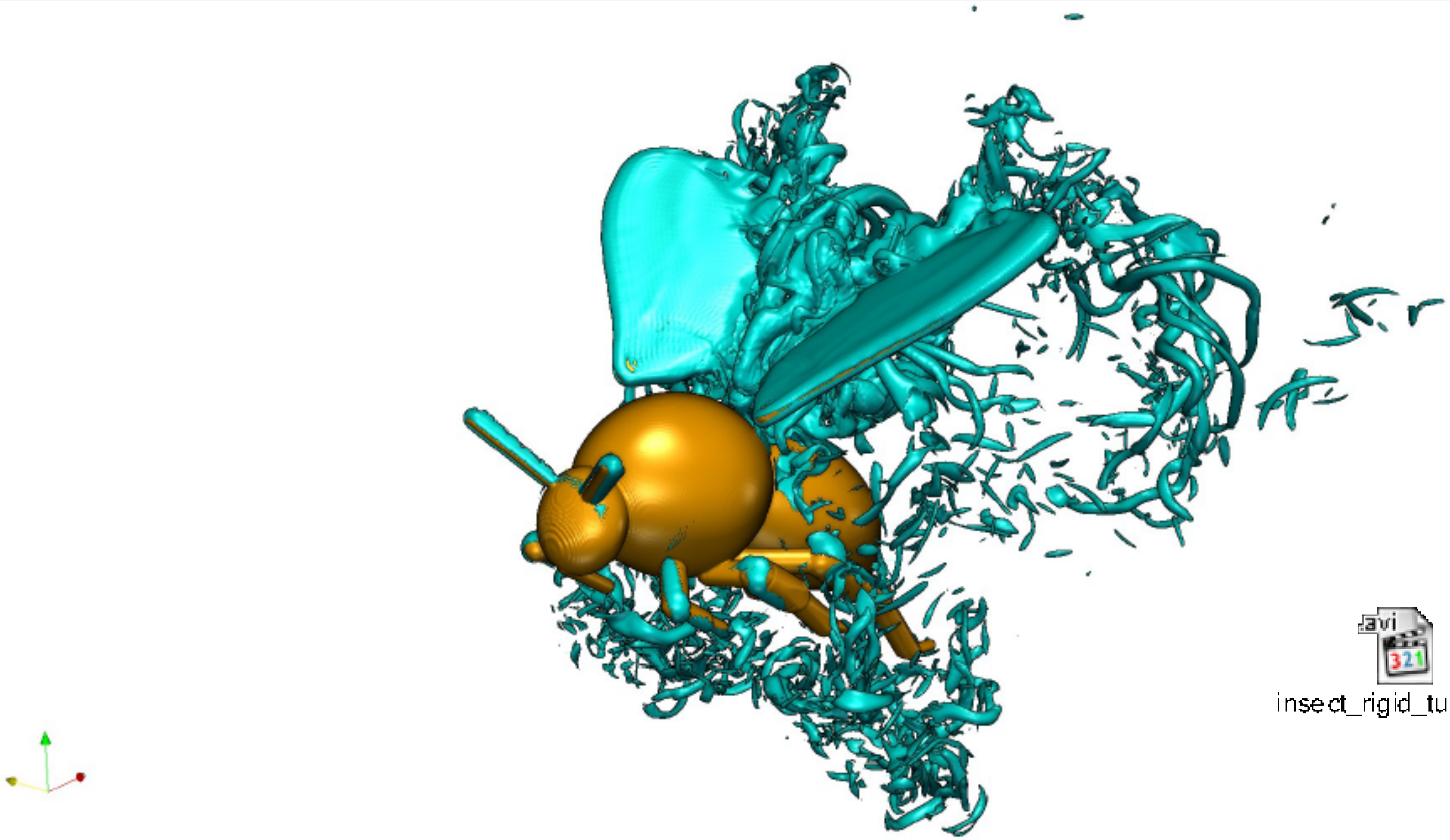

insect_rigid_turb.avi

Shown: Isosurface $||\underline{\omega}|| = 100$ Re=2042

Wake turbulence

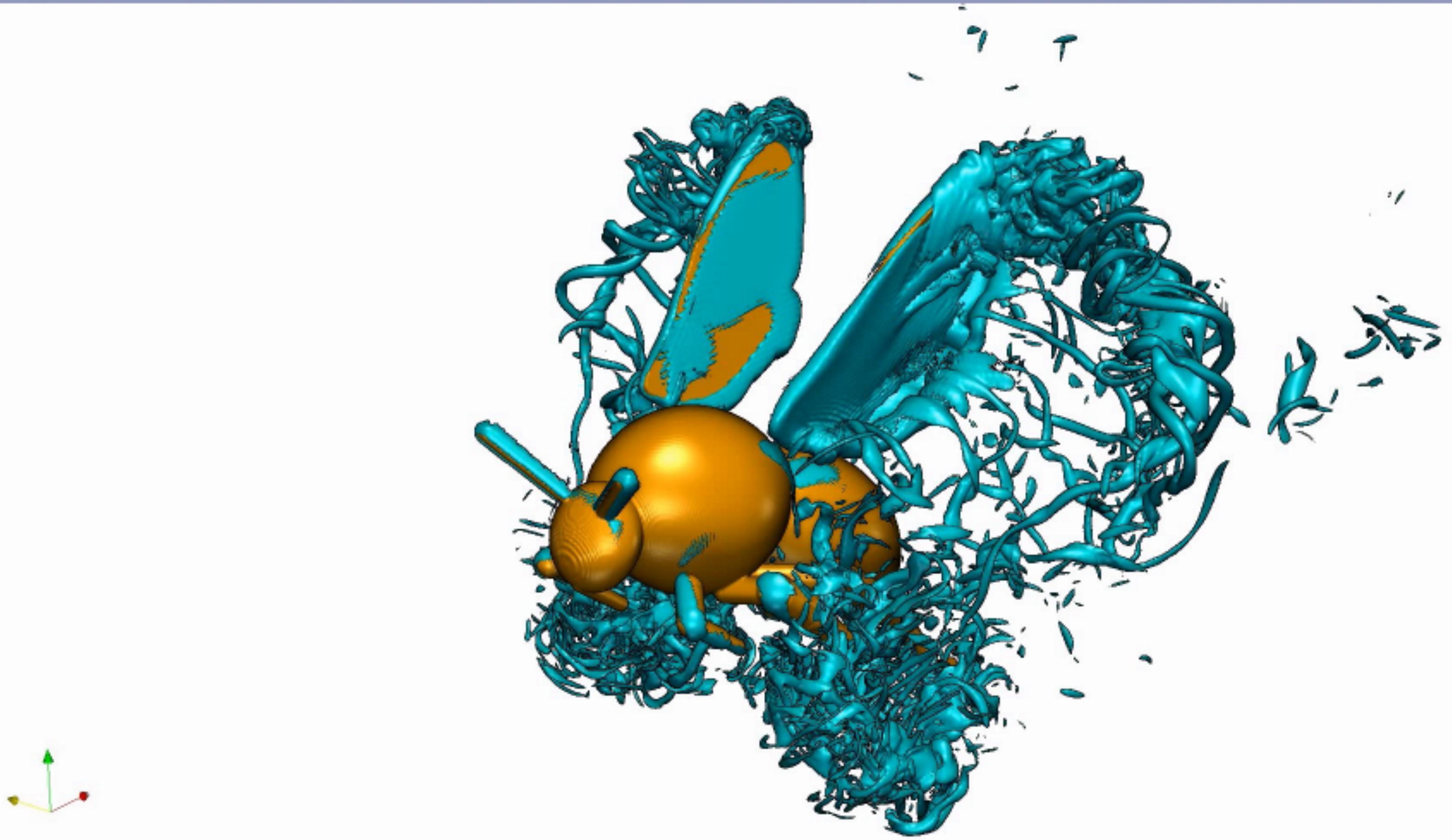

Shown: Isosurface $||\underline{\omega}|| = 100$ Re=2042

Wake Turbulence

Turbulence intensity: $\mathrm{Tu} = \underline{u}'_{\mathrm{rms}} / \underline{u}_{\infty}$

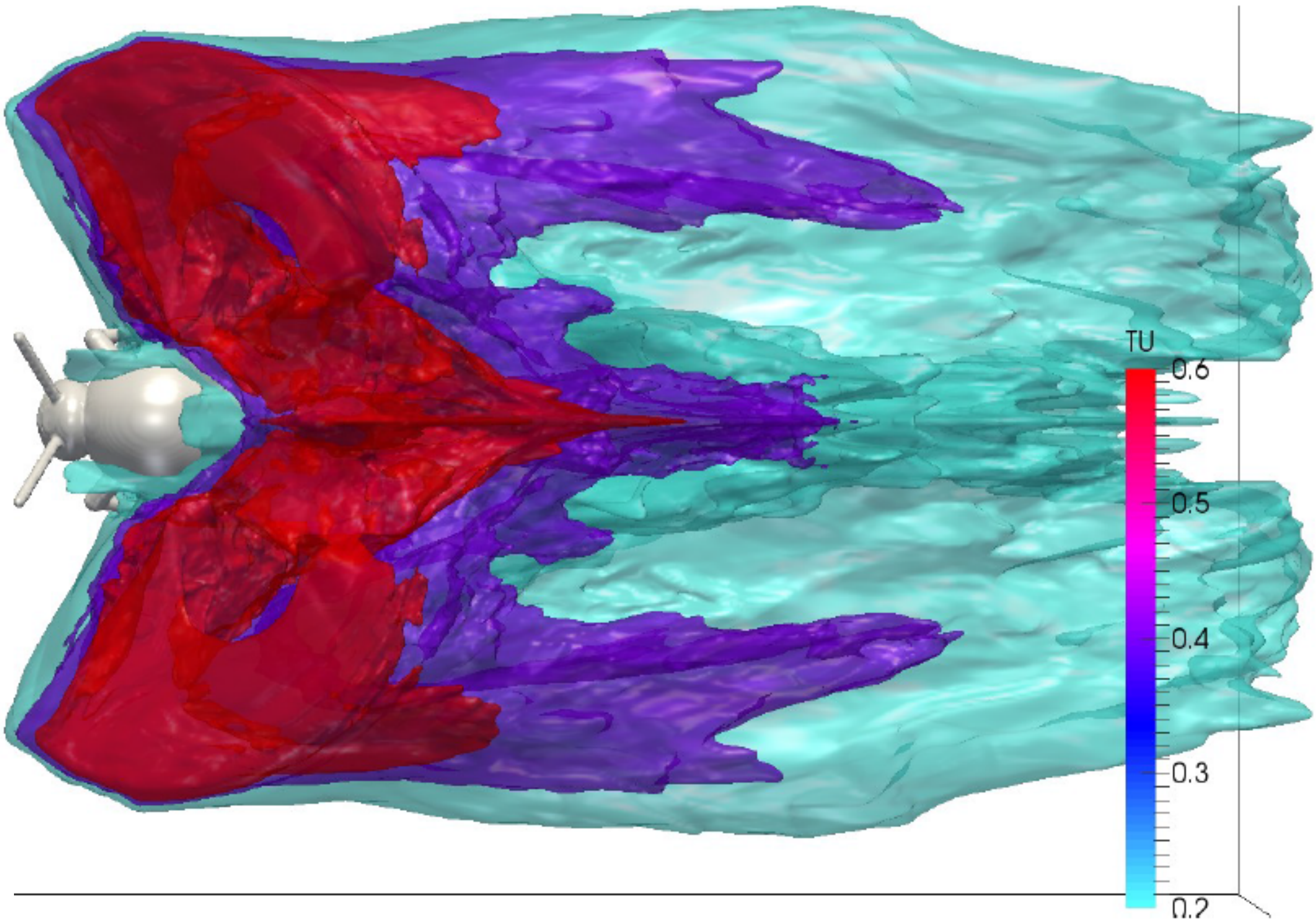

Turbulent Inflow

- Change inflow conditions to fully developed turbulence
- Model turbulence: homogeneous isotropic turbulence
- Question: do perturbations alter force production, power expenditures?
- Airfoil: turbulent transition in BL can have big effect

  T.J. Mueller, L.J. Pohlen, P.E. Conigliaro and B.J. Jansen, "The influence of Free-stream disturbances on low Reynolds number airfoil experiments", Exp. Fluids 1 (1983)

- What happens to the leading edge vortex?
- First step: tethered, uncontrolled flight

Turbulent Inflow: Setup

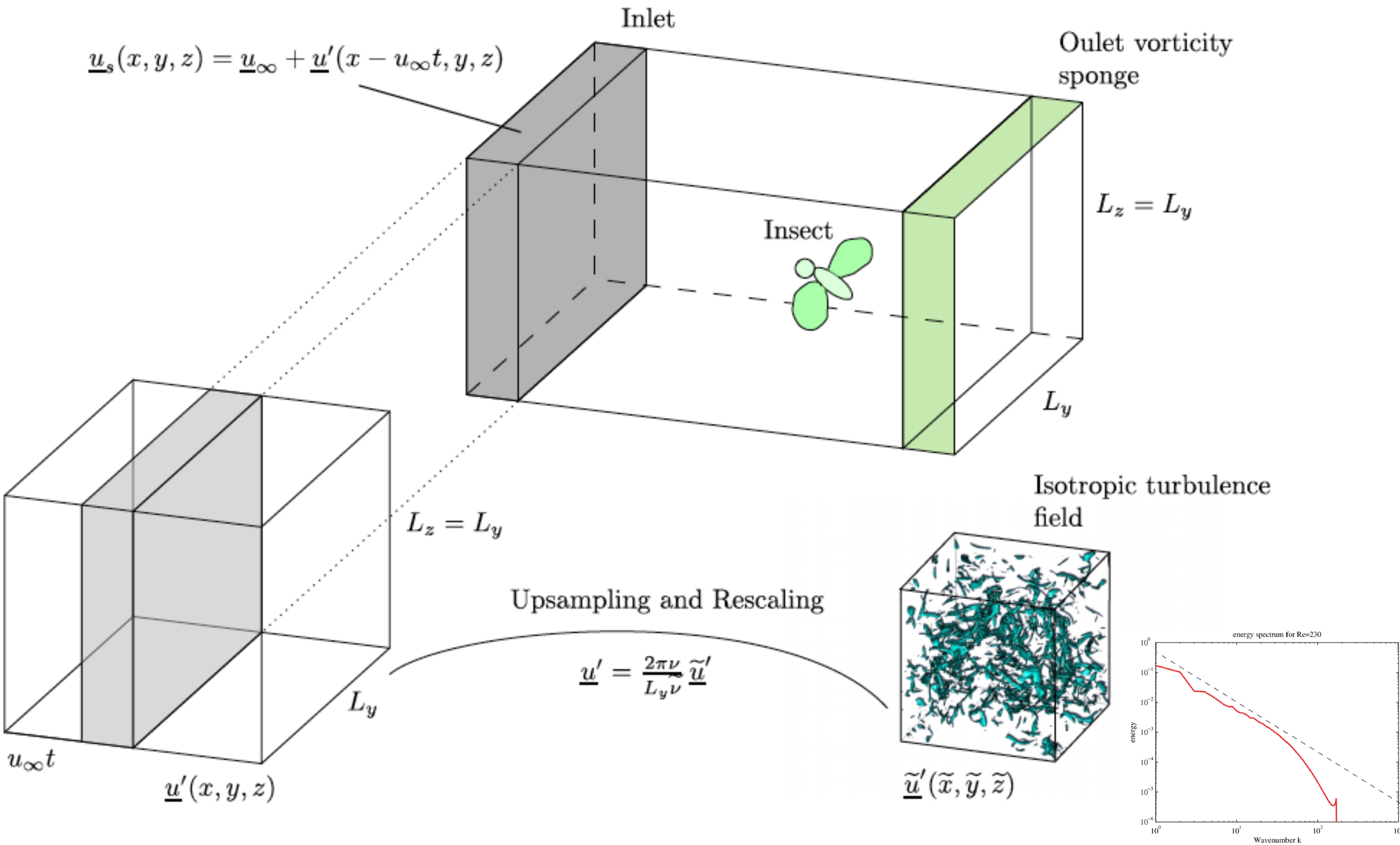

Turbulence properties

Four different inflow turbulence fields are used (dimension: R)

R_λ	Tu	ℓ_η	λ	Λ	N_W
90.5	0.17	0.013	0.246	0.772	16
130.1	0.33	0.008	0.179	0.782	16
177.7	0.63	0.005	0.129	0.759	36
227.9	0.99	0.004	0.105	0.759	108

Where: $\Lambda = \frac{\pi}{2U^2} \int_0^{k_{\max}} k^{-1} E\left(|\underline{k}|\right) \mathrm{d}k$ Integral (length)scale

$\lambda = \left(\frac{15\nu U^2}{\epsilon}\right)^{1/2}$ Taylor Micro(length)scale

$\ell_\eta = \left(\frac{\nu^3}{\epsilon}\right)^{1/4}$ Kolomogorov length scale

Flow field

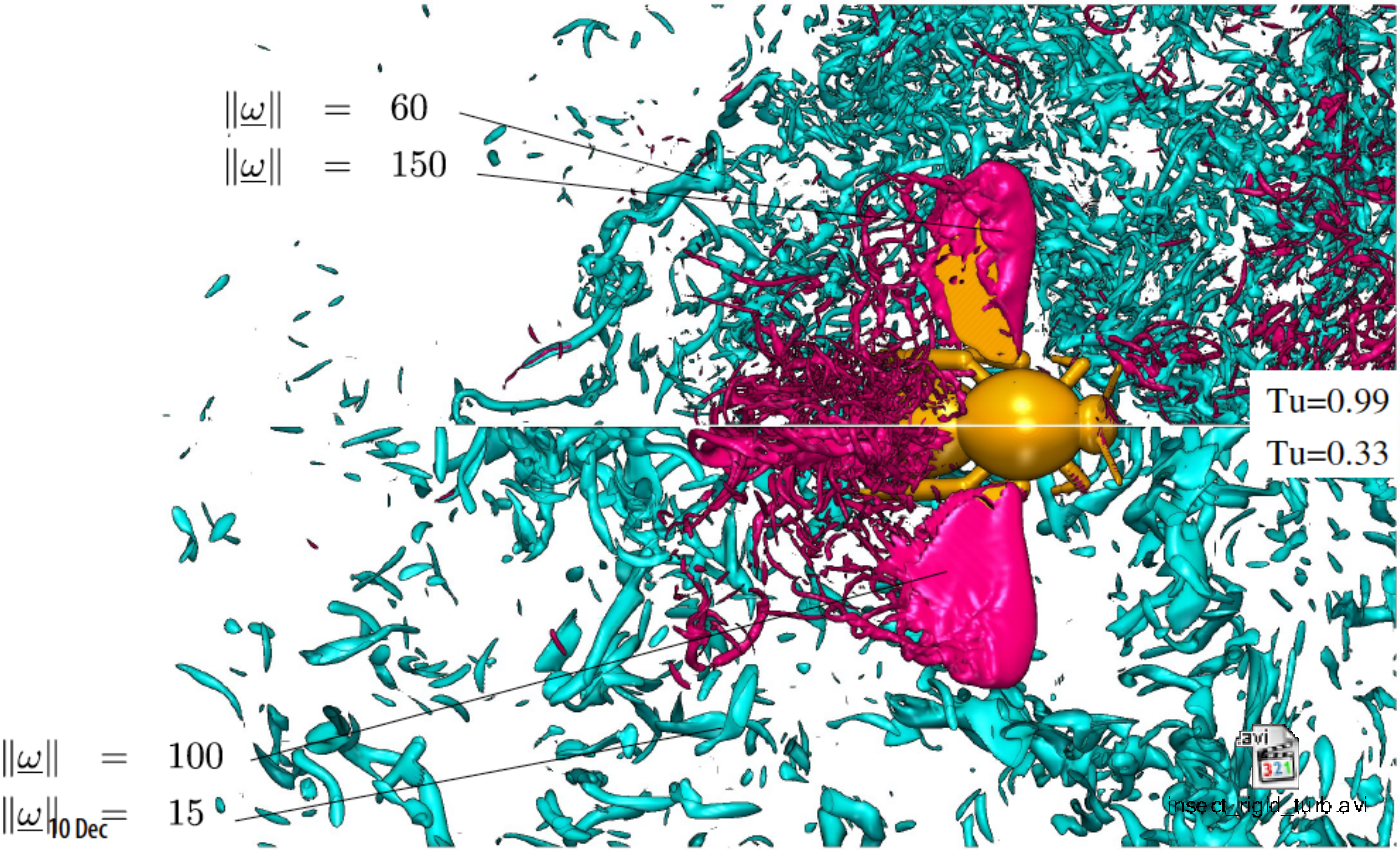

Cycle Averaged Forces/Power

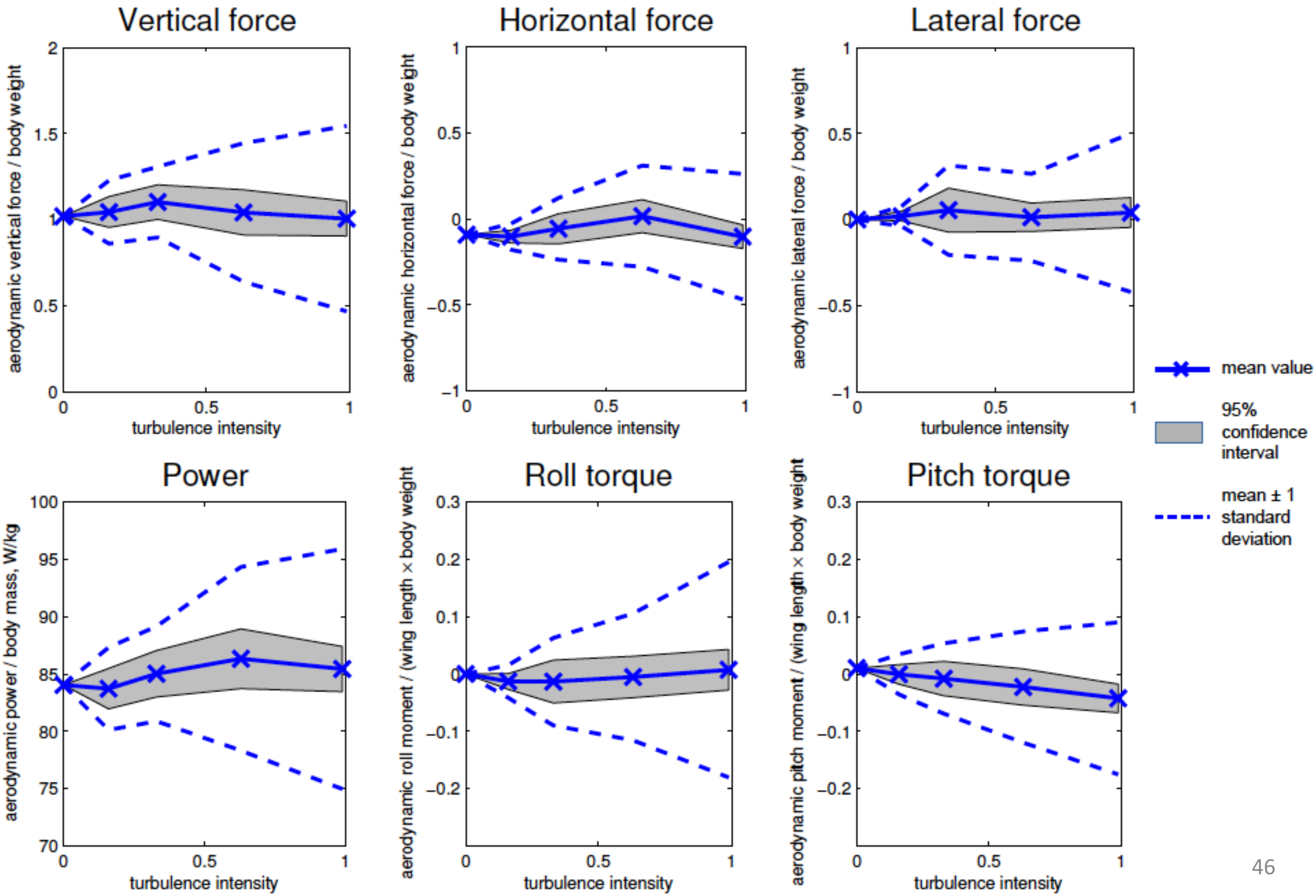

Phase averaged leading edge vortex

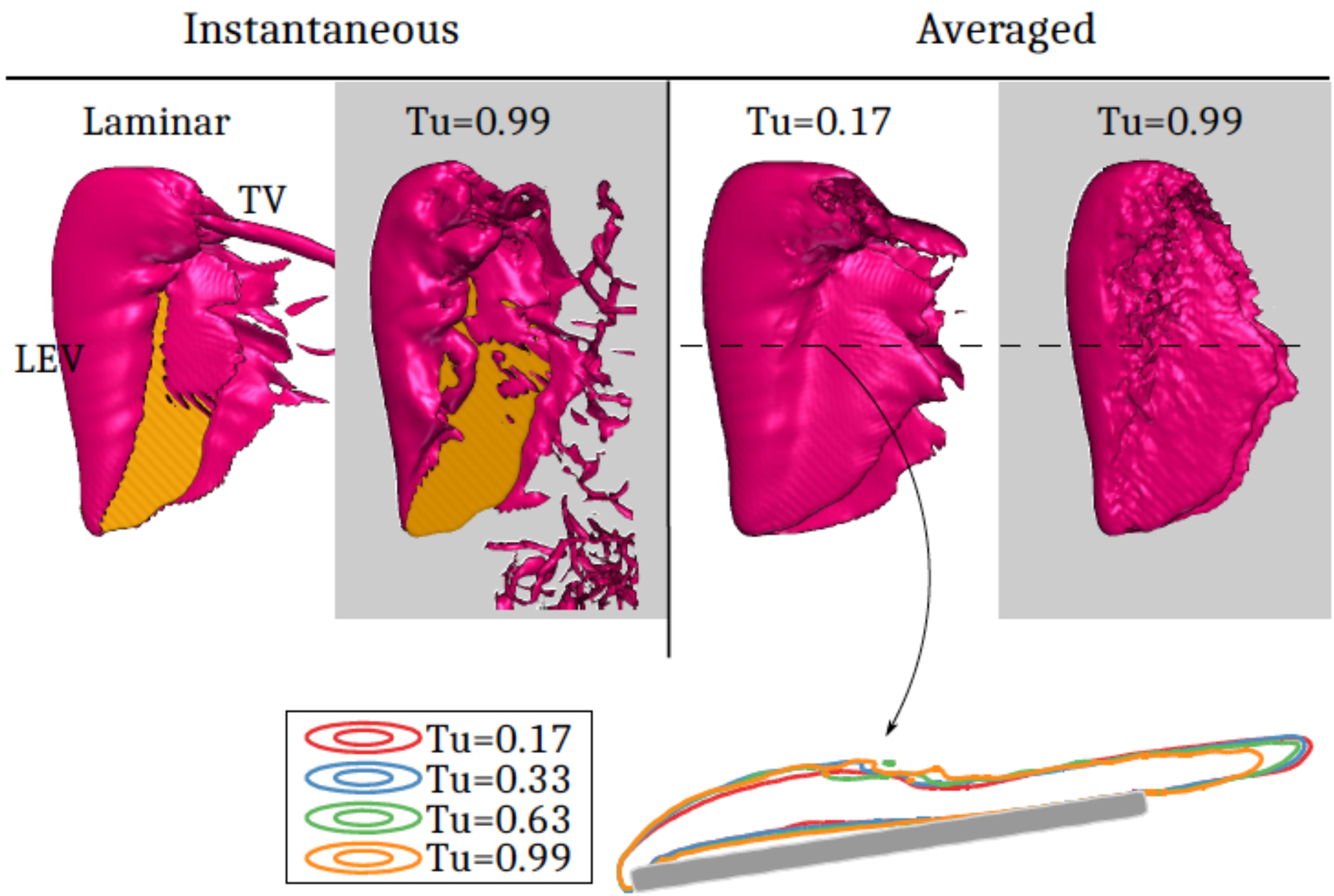

Conclusions Bumblebee

- Bumblebee model is balanced in laminar flight
- We studied turbulence intensities *Tu* up to 100%
- The forces / torques / power is on average the same, but fluctuations occur
- Different behavior in flapping flight than in airfoil-based flight (at low Re)
- Turbulence faces insects with a problem for control, not force production
- Next steps: free flight

Part III : FSI with flexible objects
Application to propulsion in water

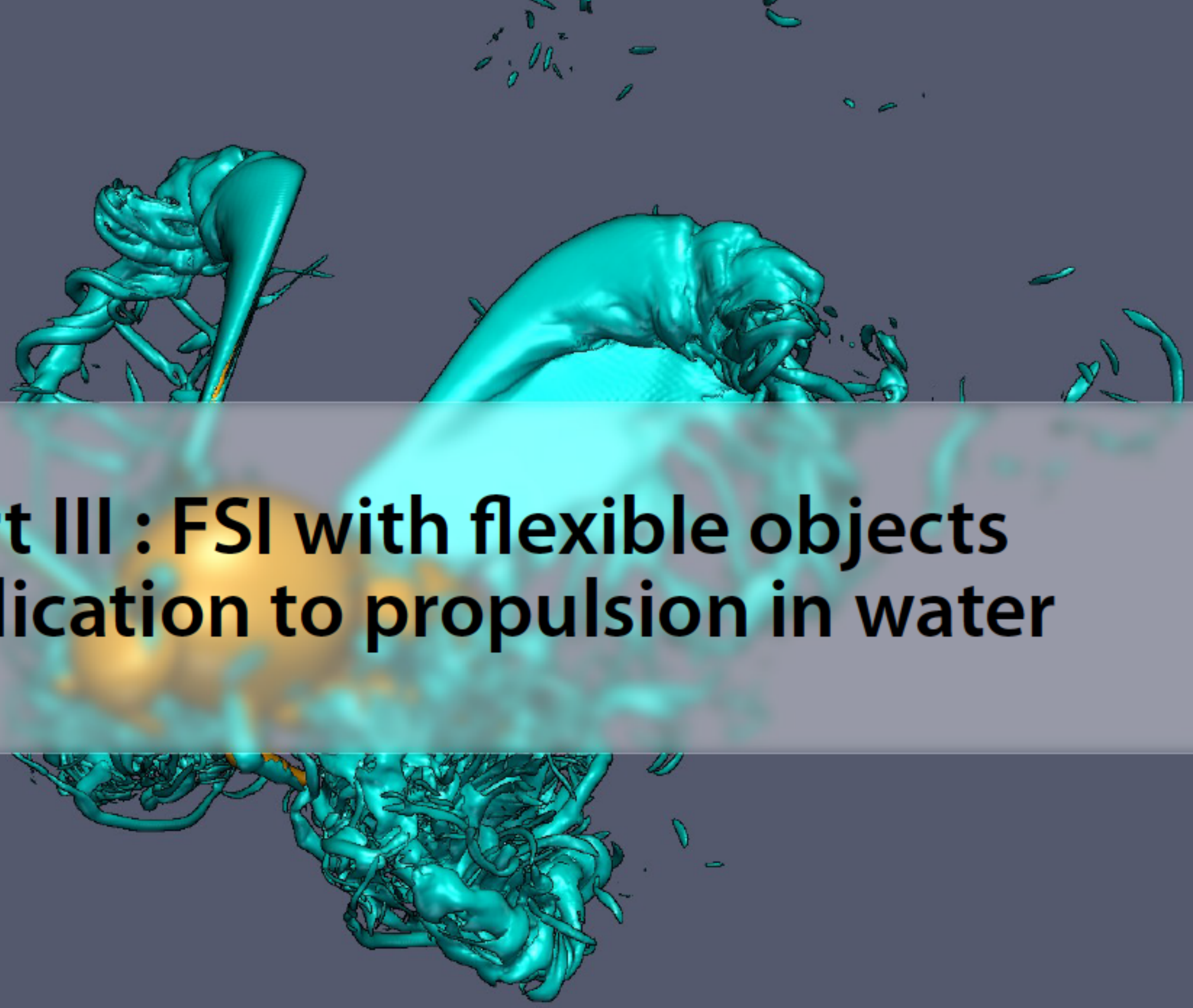

Fluid-Structure Interaction

- Insect wings are flexible
- In fact, flexibility is ubiquitous in animals
- For example: Jellyfish, insects, birds, snakes also plants
- Biological fluid-structure interaction problems typically involve large deformations

Solid Model

- 1D Beam equation
- Non-linear deflection, linear material
- Rigid in other direction
- Inextensible (incompressible)

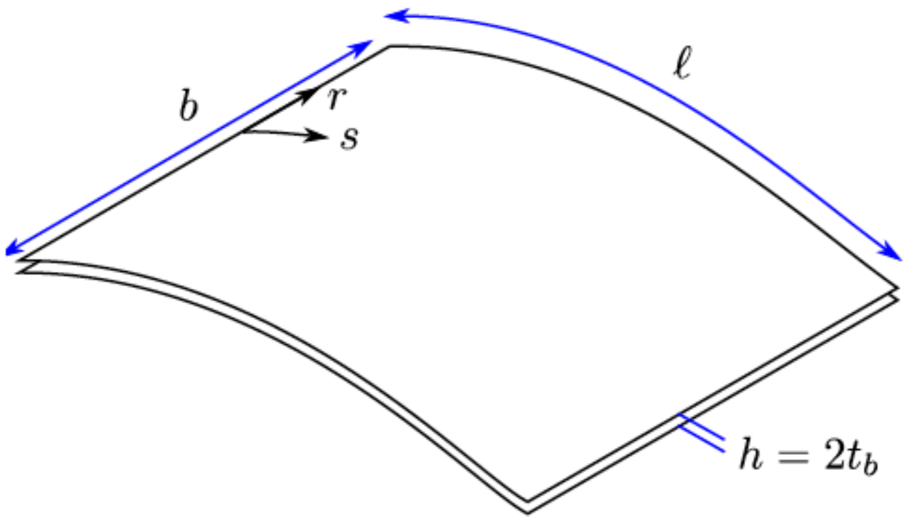

Beam Equation

Longitudinal force:

$$\frac{\partial^2 T}{\partial s^2} - T\left(\frac{\partial \Theta}{\partial s}\right)^2 = -[p]^{\pm}\frac{\partial \Theta}{\partial s} - 2\eta\frac{\partial \Theta}{\partial s}\frac{\partial^3 \Theta}{\partial s^3} - \eta\left(\frac{\partial^2 \Theta}{\partial s^2}\right)^2 \cdots$$

$$-\mu\left(\dot{\Theta} + \dot{\alpha}\right)^2 - \frac{\partial [\tau]^{\pm}}{\partial s}$$

Local deflection angle:

$$\mu\ddot{\Theta} + \mu\ddot{\alpha} + \frac{\partial [p]^{\pm}}{\partial s} = -\eta\frac{\partial^4 \Theta}{\partial s^4} + \left(T + \eta\left(\frac{\partial \Theta}{\partial s}\right)^2\right)\frac{\partial^2 \Theta}{\partial s^2} \cdots$$

$$+2\frac{\partial T}{\partial s}\frac{\partial \Theta}{\partial s} + [\tau]^{\pm}\frac{\partial \Theta}{\partial s}$$

Solved with finite differences (implicit in time)

Stiffness: $\eta = EI/\varrho_f L^3 U^2$ Density: $\mu = \varrho_s A/\varrho_f L^2$

S. Michelin and S. Llewellyn Smith and B. Glover, "Vortex shedding model of a flapping flag", J. Fluid Mech. (2008)

Coupling: Time Marching

Semi-implicit algorithm (good for aeroelasticity)

Require: Fluid velocity field $\underline{\mathsf{u}}^{\mathsf{n}}$ and solid state $\mathcal{S}^{\mathsf{n}}$ at time t^{n}

1: Construct mask function χ^{n} and solid velocity field $\underline{\mathsf{u}}_{\mathsf{s}}^{\mathsf{n}}$ from solid state $\mathcal{S}^{\mathsf{n}}$

2: Compute source terms for the fluid $\underline{\mathsf{f}}^{\mathsf{n}} = \underline{\mathsf{f}}(\underline{\mathsf{u}}^{\mathsf{n}}, \chi^{\mathsf{n}}, \underline{\mathsf{u}}_{\mathsf{s}}^{\mathsf{n}})$

3: Advance fluid to new time level $\underline{\mathsf{u}}^{\mathsf{n}} \rightarrow \underline{\mathsf{u}}^{\mathsf{n}+1}$ using the AB2 scheme

4: Compute static pressure $\mathsf{p}^{\mathsf{n}+1} = \mathsf{p}(\underline{\mathsf{u}}^{\mathsf{n}+1}, \chi^{\mathsf{n}}, \underline{\mathsf{u}}_{\mathsf{s}}^{\mathsf{n}})$

5: Interpolate pressure jump $[\mathsf{p}]^{\pm}(\mathsf{t}^{\mathsf{n}+1}) = \mathcal{I}(\mathsf{p}^{\mathsf{n}+1})$

6: Advance solid state $\mathcal{S}^{\mathsf{n}} \rightarrow \mathcal{S}^{\mathsf{n}+1}$ using $[\mathsf{p}]^{\pm}(\mathsf{t}^{\mathsf{n}+1})$ and the BDF2 scheme

7: **return** New fluid state $\underline{\mathsf{u}}^{\mathsf{n}+1}$ and new solid state $\mathcal{S}^{\mathsf{n}+1}$

Swimmer

- Swimmer model: pitching plate
- Chordwise flexible and spanwise rigid
- Swimmer tethered but meanflow free
- Experimental work with Mylar sheet

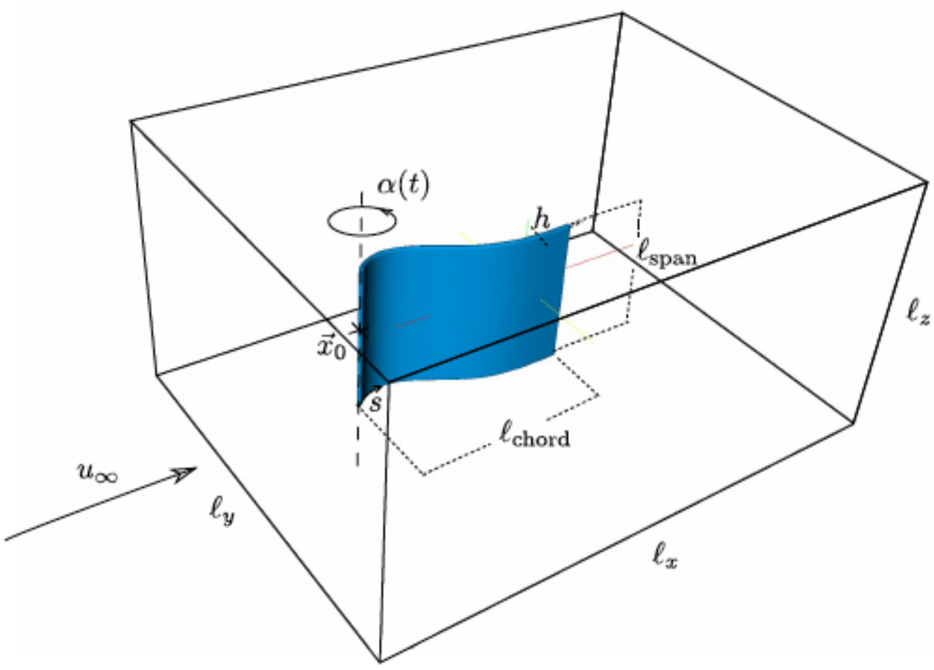

Raspa et al.: "Vortex-induced drag and the role of aspect ratio in undulatory swimmers." Phys. Fluids, 2014

Flow field

Isosurfaces of vorticity $\|\underline{\omega}\| = 18$(copper), $\|\underline{\omega}\| = 9$(blue)

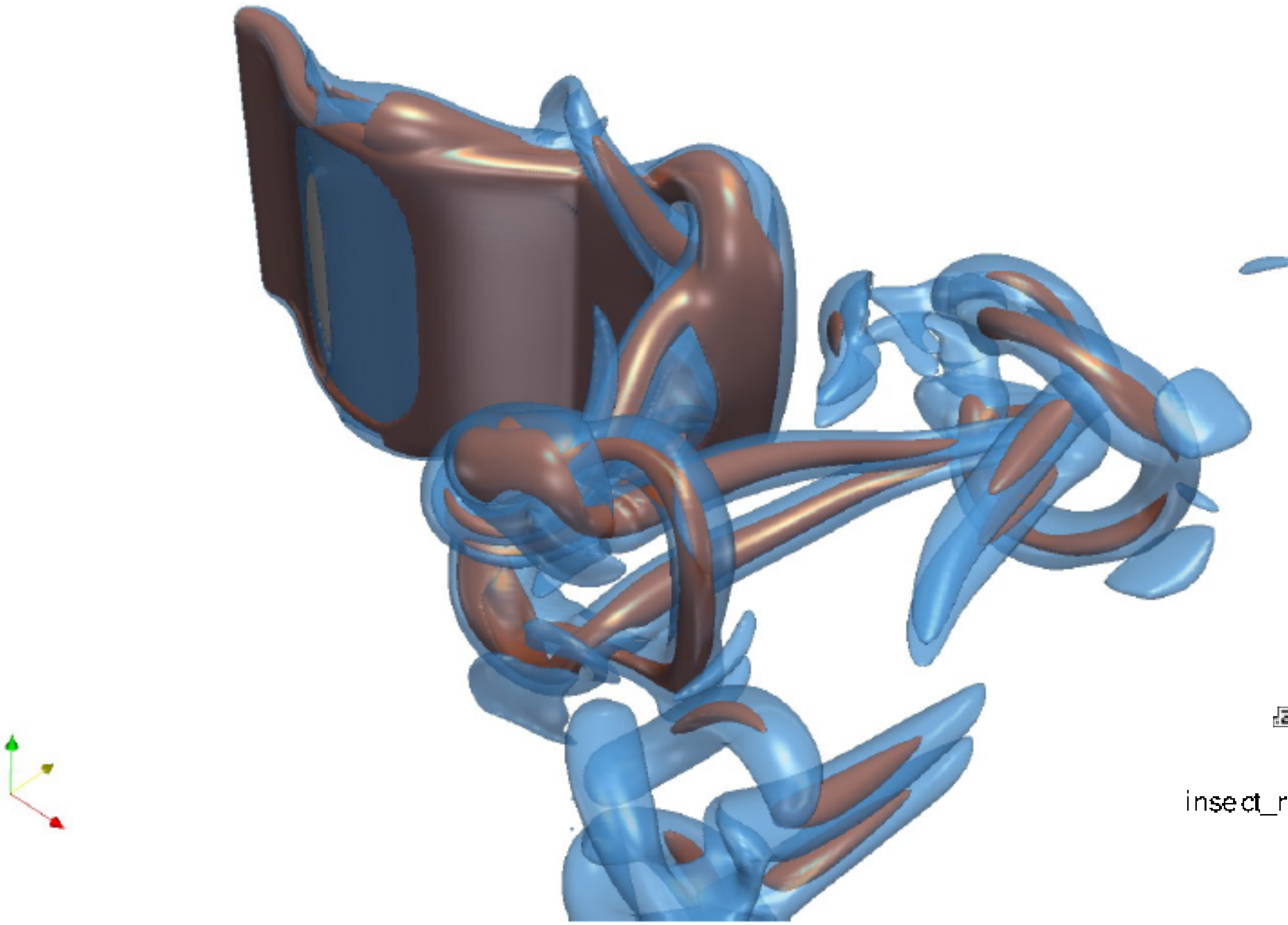

insect_rigid_turb.avi

Influence of the Aspect Ratio

- First step: vary aspect ratio, keeping velocity fixed
- Driving motion: $\alpha = 50^\circ \sin(2\pi \mathsf{f} \mathsf{t})$
- $\mathrm{Re} = \mathsf{R}^2 \mathsf{f}/\nu = 1000$
- Ansatz:

$$\mathsf{F}_\mathsf{x}^{3D} = \mathsf{F}_{\mathrm{thrust}} \cdot \mathsf{AR} + \mathsf{F}_{\mathrm{tip}}$$
$$\mathsf{F}_\mathsf{x}^{2D} = \mathsf{F}_{\mathrm{thrust}}^{2D} \cdot \mathsf{AR}$$

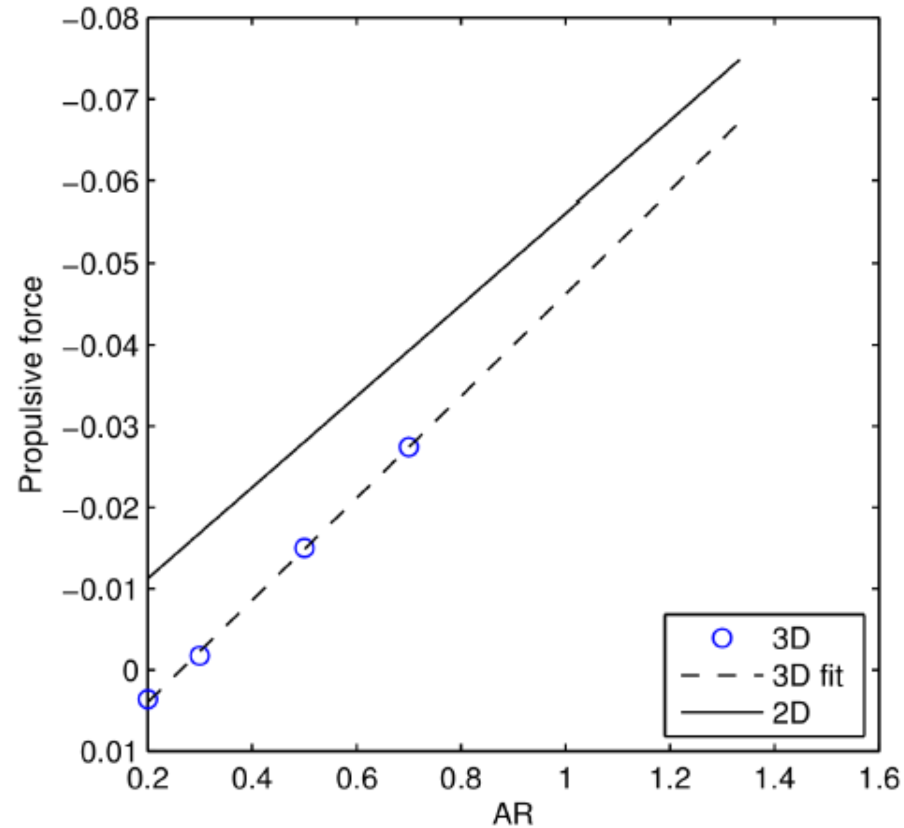

→ the tip vortices are responsible for a part of the drag and thus influence the cruising speed

Non-rectangular shapes

Inspiration: fish caudal fins are very differently shaped

We choose three shapes with the same surface

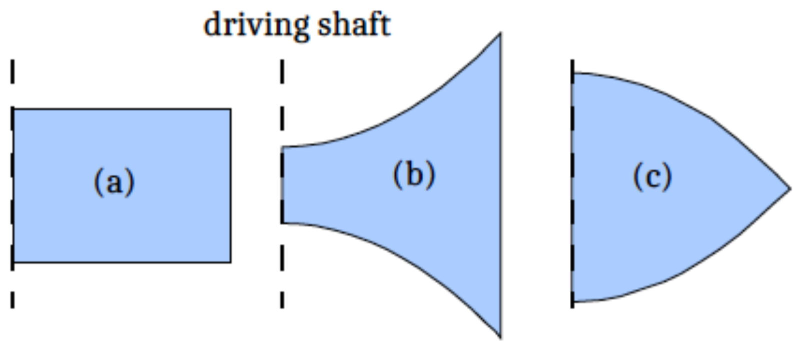

What is the influence of the shape on the tip vortices?

Swimmer Race

- Same Re and driving motion
- We assume constant material properties
- Swimmers accelerate the fluid
- Contracting shape outruns others

Re=1000

$\alpha = 50^\circ \sin\left(2\pi f\right)$

$512 \times 384 \times 256$

Accelerate fluid and keep swimmer fixed:

$$\frac{\mathrm{d}}{\mathrm{d}t} u_\infty^{(x)} = \frac{\left\langle -\frac{\chi}{\varepsilon} \left(\underline{u} - \underline{u}_s\right)\right\rangle}{m_{\text{fluid}}}$$

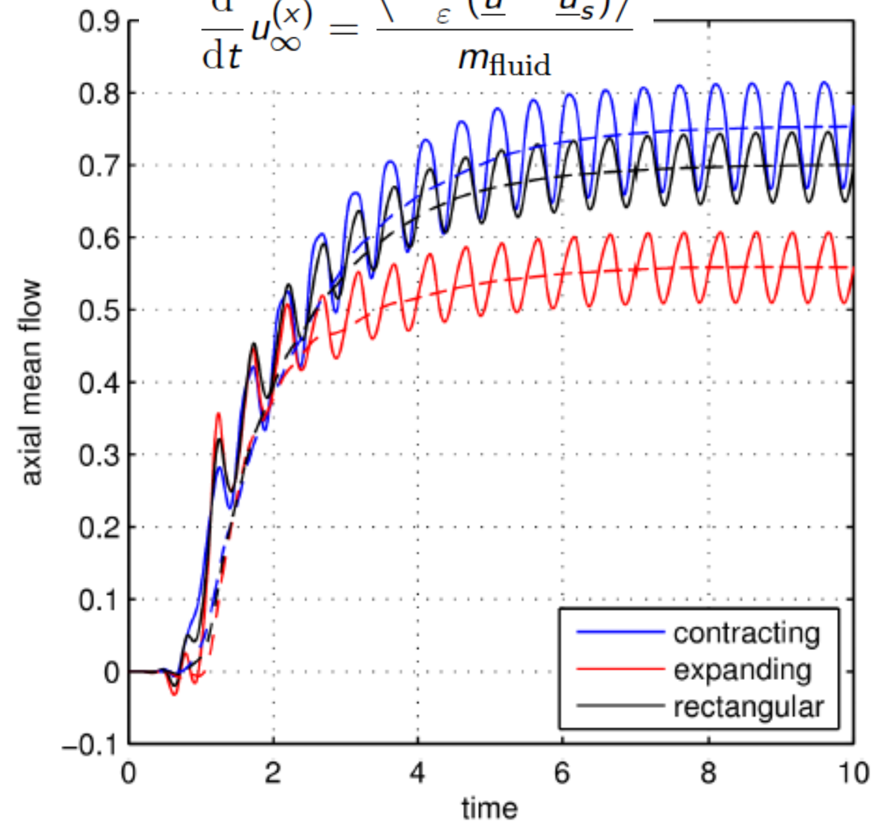

Contracting Shape

Isosurfaces of vorticity $||\underline{\omega}|| = 18(\text{purple}), ||\underline{\omega}|| = 9(\text{blue})$

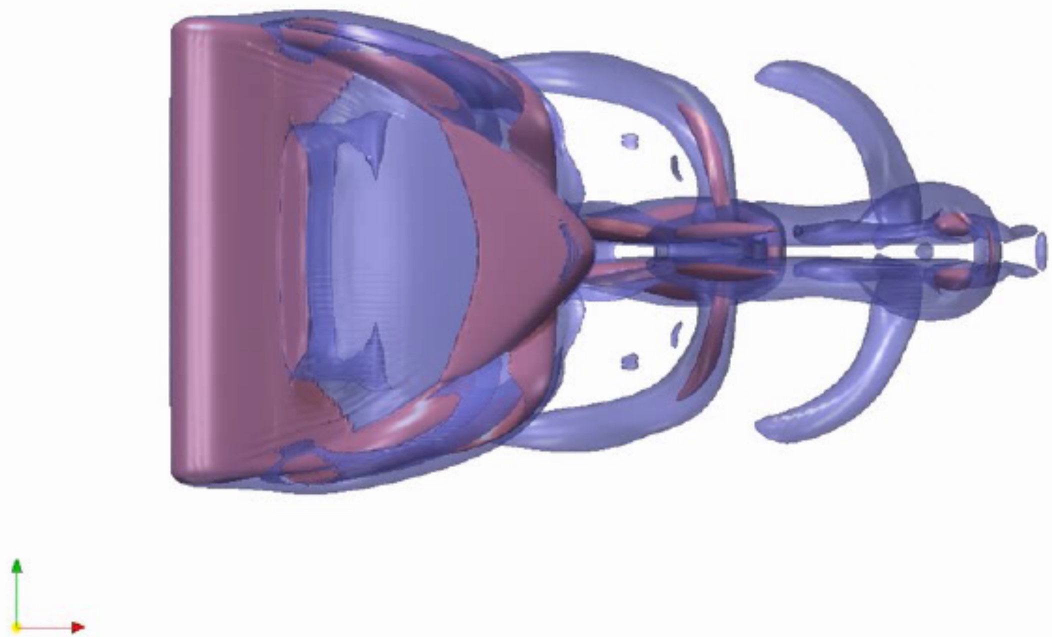

insect_rigid_turb.avi

Expanding Shape

Isosurfaces of vorticity $||\underline{\omega}|| = 18$(purple), $||\underline{\omega}|| = 9$(blue)

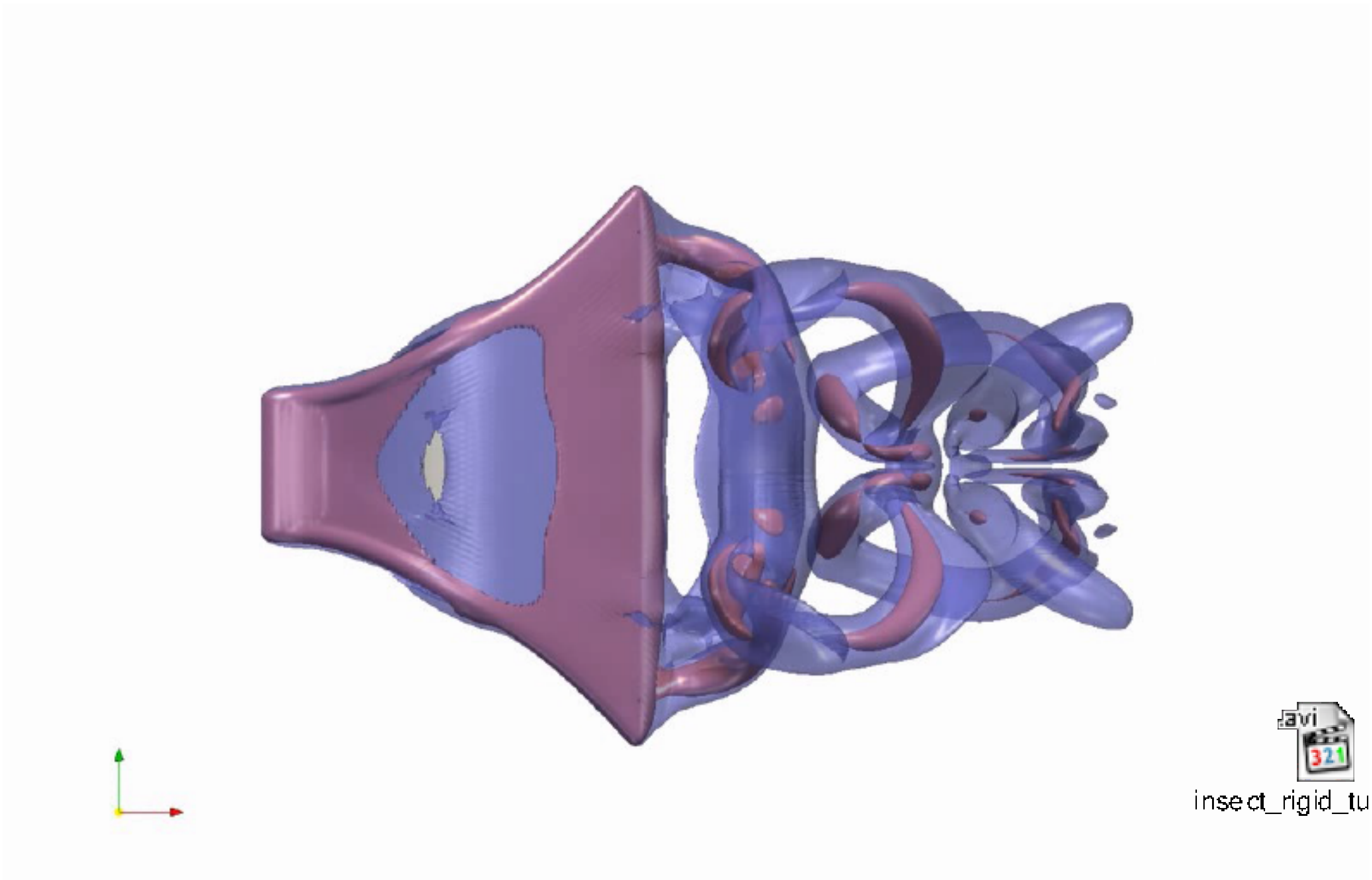

insect_rigid_turb.avi

Expanding vs contracting shape

Contracting swims faster and consumes less power

Shape	u_∞	P_{aero}	Trailing edge displacement
contracting	0.75	0.16	0.62
expanding	0.56	0.21	0.42

Trailing edge displacement is different: prescribe contracting motion with expanding shape and vice-versa

→ contracting shape is still better

Rigid plates: expanding faster but less efficient

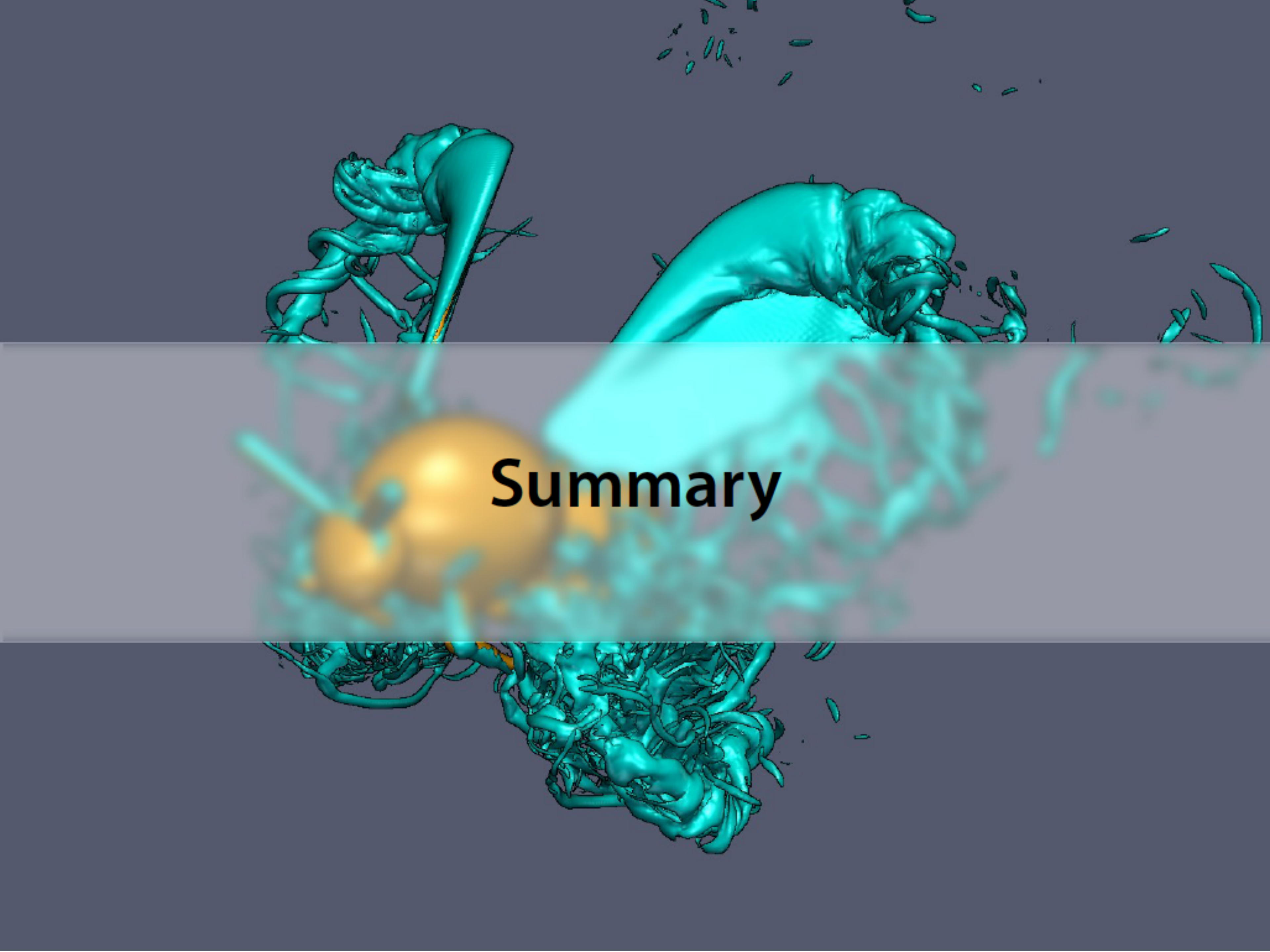
Summary

Aix*Marseille université

Summary

- Numerical method based on Fourier and volume penalization fruitful combination for a wide range of application
- Based on previous 2D work for moving rigid obstacles
- New open-source code FLUSI
- Newly designed insect module
- Validation tests show good agreement
- Spectral differentiation advantageous if fine structures appear (Turbulence, Elevated Reynolds number)
- Evolution from rigid to flexible obstacles using the volume penalization method

Summary

- We studied a Bumblebee model in turbulent inflow
  - Wake turbulence gives an idea about relevant intensities
  - Consider homogeneous isotropic turbulence as model
  - Inflow perturbations did not alter statistically averaged forces
  - Leading edge vortex intact in averaged sense
- We devised 1D flexibility model for 3D FSI
  - Application to swimming: contracting shape found better than expanding shape
  - Conjecture: tip vortices are interacting differently with surface

References

T. Engels, D. Kolomenskiy, K. Schneider, F.O. Lehmann and J. Sesterhenn.
Bumblebee flight in heavy turbulence.
Phys. Rev. Lett., 116, 028103, 2016.

T. Engels, D. Kolomenskiy, K. Schneider and J. Sesterhenn.
FluSI: A novel parallel simulation tool for flapping insect flight using a Fourier method with volume penalization. *SIAM J. Sci. Comput., accepted*, 04/2016, arXiv:1506.06513

K. Schneider.
Immersed boundary methods for numerical simulation of confined fluid and plasma turbulence in complex geometries: a review. *J. Plasma Phys.*, 81(6), 435810601, 2015.

R. Nguyen van yen, D. Kolomenskiy and K. Schneider.
Approximation of the Laplace and Stokes operators with Dirichlet boundary conditions through volume penalization: a spectral viewpoint. *Numer. Math.*, 128:301-338, 2014.

Outlook – Ongoing Work

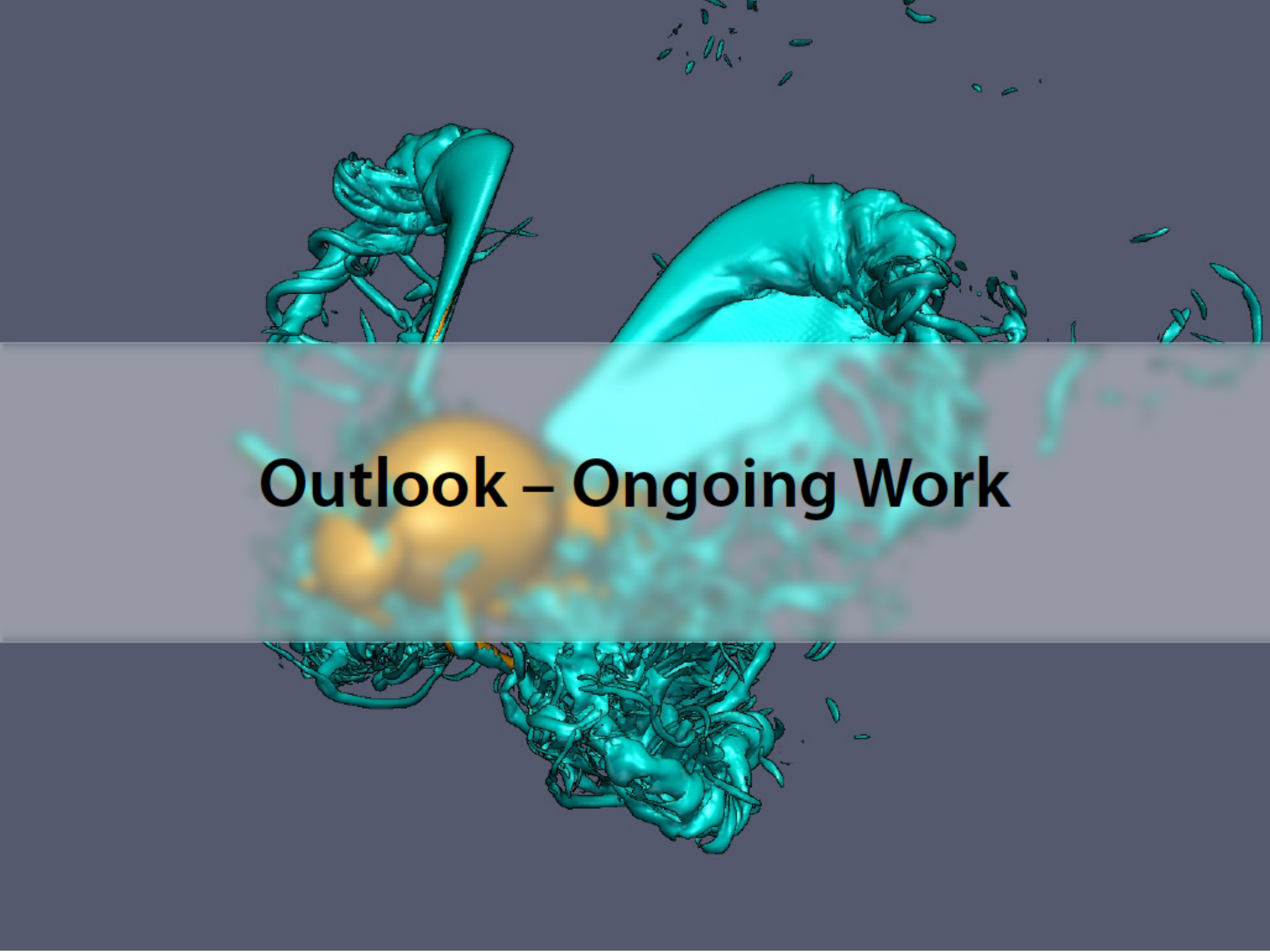

Body dynamics of a bumblebee in forward flight

Wind tunnel experiment by S. Ravi et al.

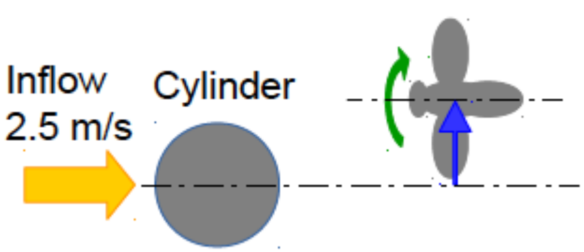

Lateral displacement

Roll angle

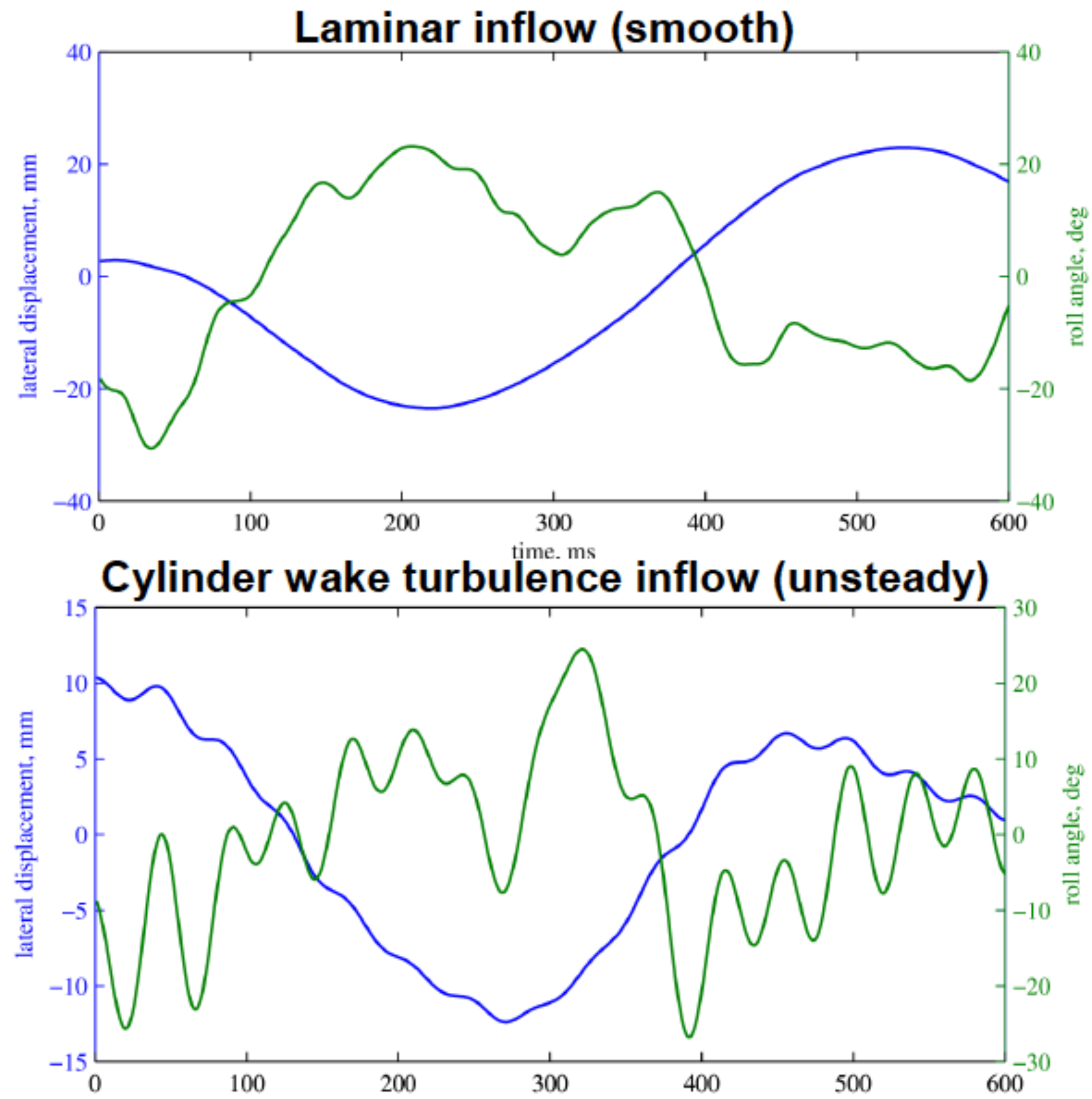

Flow visualization (vorticity magnitude)

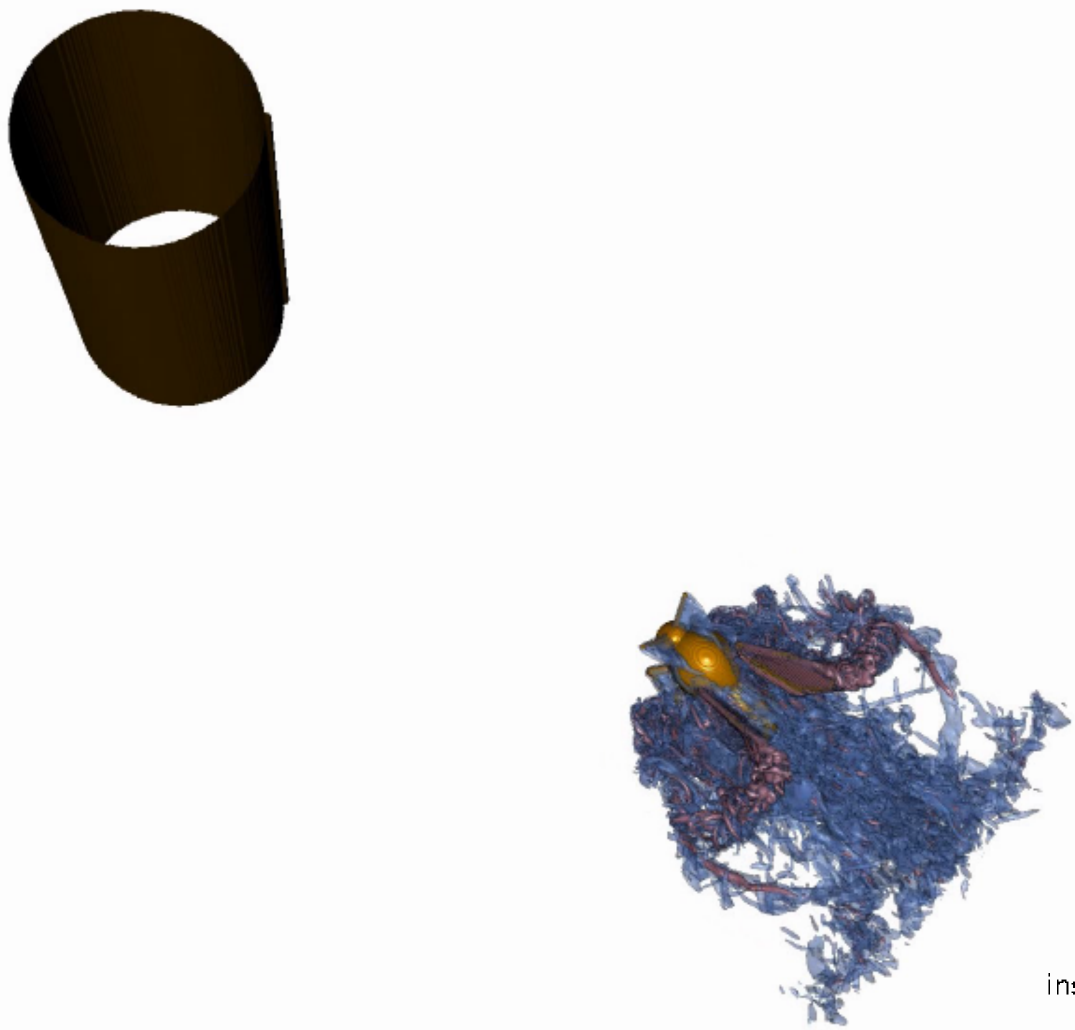

insect_rigid_turb.avi

Thank you very much for your attention!